Quaternaire, **30**, (2), *2020*, p. 91-116

THE GIANT QUATERNARY BALLIK TRAVERTINE SYSTEM IN THE DENIZLI BASIN (SW TURKEY): A PALAEOENVIRONMENTAL ANALYSIS

Cihan ARATMAN[1,2*], Mehmet ÖZKUL[2], Rudy SWENNEN[1*], Cathy HOLLIS[4], Marcelle MARQUES ERTHAL[3], Hannes CLAES[5] & Zahra MOHAMMADI[1]

ABSTRACT

This research forms the basis for the applicability of the Dunham (1962) classification of carbonated rock lithofacies to the analysis of the giant Ballık travertine architecture, while reconstructing lateral and vertical environmental changes. This study provides an analogue for spring-related deposits encountered offshore Brazil and Angola by linking macroscopically travertine lithofacies distribution to depositional environments. The analysis is based on rock-building constituents such as gastropods, charophytes, intraclasts, phytoclasts, coated grains, dendrites etc., forming micro-sedimentary fabrics with different structures such as packstone, grainstone, wackestone and boundstone, these latter closely associated with crust of dendrites and phytoherm of reeds and bryophytes. Our findings indicate that the Ballık travertine area consists of a "Lower" and an "Upper Domain" reflecting different depositional environments. More specifically, the "Lower Domain" consists from west to east of a laterally complex amalgamation of extended pool, marsh pool and flood plain environments that formed from a mixture of spring and ground waters. The extended pond environment characterised by a boundstone facies of stromatolites in the west evolves eastward into a marsh pool and flood plain. This is because CO_2 degassing and water temperature decreased as the water depth of the Lower Domain reduced towards the east. The marsh pool environment includes packstone to grainstone lithofacies and abundant wackestone lithofacies made of phytoclasts, whose crusts exhibit pustular fabrics. Moreover, the flood plains along with the marsh pool consist dominantly of packstone to grainstone lithofacies with many gastropods and intraclasts, interfingered with wackestone lithofacies made of phytoclasts. Irregular clotted fabrics, along with coated grains with radial fibres, high lime mud content with bioturbation are also present. The "Upper Domain" displays a laterally less heterogeneous palaeoenvironmental distribution with flooded slope and flood plain deposits. The eastern part of the "Upper Domain" is characterized by a systematic alternation of these environments, with intercalations of wackstone lithofacies made of phytoclasts, packstone to grainstone lithofacies made of intraclasts and lime muds as well as coated grains. The flood plain has coated grains having peloidal nuclei and coatings of sparry laminations and clotted fabric of peloids representing intraclasts, whereas, the flooded slope possesses coated grains with coatings of dendrites and nuclei of peloids, boundstone of stromatolites which have flat-laminated and columnar-laminated fabrics indicating a laminar discharge away from the spring(s). Alluvial fan and palustrine deposits with abundant bryophytes and reeds frequently interfinger with marsh pool environment in the "Lower Domain", and with the flood plain and flooded slope environments in the "Upper Domain". The results illustrate well how environmental changes identified in the two different domains have induced heterogeneity in reservoir-based depositional architecture.

Keywords: travertine, depositional environment, Dunham lithofacies, fabric, Turkey

RÉSUMÉ

LE SYSTÈME DE TRAVERTIN QUATERNAIRE GÉANT DE BALLIK DANS LE BASSIN DE DENIZLI (SUD-OUEST DE LA TURQUIE) : UNE ANALYSE PALÉOENVIRONNEMENTALE

Cette recherche s'appuie sur l'analyse des lithofaciès du travertin quaternaire de Ballık en utilisant le système de classification pour les roches carbonatées de Dunham (1962), tout en reconstituant les changements environnementaux latéraux et verticaux. Cette étude fournit un analogue pour les dépôts de source rencontrés au large du Brésil et de l'Angola en établissant un lien entre la distribution macroscopique des lithofaciès de travertin et les environnements sédimentaires. L'analyse des lithofaciès est basée sur l'étude microscopique des roches tels que les gastéropodes, charophytes (algues vertes), intraclastes, phytoclastes, grains enrobés, dendrites, etc., formant des tissus micro-sédimentaires liés entre eux durant le dépôts (*boundstone*), dont le faciès est étroitement associé à la croûte de dendrites et au phytohermes de roseaux et de bryophytes, ou constitué postérieurement et dont la structure est alors caractérisée par l'absence d'une matrice de particules fines (*grainstone*) ou une présence modérée, laissant les grains jointifs (*packstone*), à élevée (*wackestone*), les grains étant alors non-jointifs. Nos résultats indiquent que la zone de travertin de Ballık se compose d'un « Domaine inférieur » et d'un « Domaine supérieur » reflétant différents environnements de dépôts. Plus précisément, le Domaine inférieur consiste d'ouest en est en une amalgamation latéralement complexe d'environnements de lacs, de marais et de

[1] Geodynamics and Geofluids Research Group, Department of Earth and Environmental Sciences, KU Leuven, Celestijnenlaan 200E, BE-3001 LEUVEN. *Emails*: cihan.aratman@kuleuven.be, rudy.swennen@kuleuven.be
[2] Department of Geological Engineering, Pamukkale University, Kınıklı Campus, 20070, DENIZLI, TURKEY. *Email*: mozkul@pau.edu.tr
[3] Petrobras Research Center, Av. Horacio de Macedo Cidade Universitaria, 950, Ilha do Fundao, 21941-915 RIO DE JANEIRO, BRAZIL. *Email*: marcellerthal@gmail.com
[4] Department of Earth and Environmental Sciences, University of Manchester, Williamson Building, 2.69, Oxford Road, MANCHESTER M13 9PL. *Email*: cathy.hollis@manchester.ac.uk
[5] Clay and Interface Mineralogy, Energy & Mineral Resources, RWTH Aachen University, 18 Bunsenstrasse 8, DE-52072 AACHEN. *Email*: hannes.claes@emr.rwth-aachen.de

Manuscrit reçu le 14/12/2019, accepté le 29/06/2020

plaines inondables qui se sont formés à partir d'un mélange d'eaux de source et d'eaux souterraines. L'environnement de remplissage lacustre incluant des stromatolites à l'ouest évolue vers l'est en un marais et une plaine inondable. En effet, le dégazage du CO_2 et la température de l'eau ont diminué à mesure que la tranche d'eau du Domaine inférieur diminuait vers l'est. L'environnement de marais comprend des lithofaciès de type *packstone* à *grainstone* et un lithofaciès abondant de type *wackestone* de phytoclastes, dont les croûtes présentent des structures pustuleuses. De plus, les plaines inondables ainsi que le bassin marécageux se composent principalement de lithofaciès de type *packstone* à *grainstone* avec de nombreux gastéropodes et intraclastes, entrecoupés de faciès *wackestone* à phytoclastes. On note également une fabrique grumeleuse irrégulière, accompagnée de grains à structure fibreuse radiale et revêtements, une teneur élevée en boue calcaire et la présence de bioturbations. Le « Domaine supérieur » présente une distribution paléoenvironnementale latéralement moins hétérogène avec des dépôts de pente inondée et de plaines d'inondation. La partie orientale du « Domaine supérieur » se caractérise par une alternance systématique de ces environnements, avec des intercalations de lithofaciès, de type *wackestone* à phytoclastes et *packstone* to *grainstone* à intraclastes, et de boues calcaires ainsi que de grains enrobés. Les dépôts de plaine d'inondation sont constitués de grains formés d'un noyau de peloïdes et d'un revêtement de laminations sparitiques, organisés en une fabrique grumeleuse d'intraclastes, alors que les dépôts de pente inondée incluent des grains enrobés de dendrites et noyaux en peloïdes et fragments de stromatolithes, dont les fabriques sont à laminations plates et en colonne indiquant un écoulement laminaire éloigné des sources. Les dépôts alluviaux en éventail et palustres riches en bryophytes et roseaux interfèrent fréquemment avec les environnements de marécage dans le « Domaine inférieur », et avec les environnements de la plaine d'inondation et de pentes dans le « Domaine supérieur ». Les résultats illustrent bien comment des transitions environnementales irrégulières, qui se reflètent dans différents domaines, induisent une hétérogénéité dans la structure du gisement.

Mots-clés : travertin, milieux de dépôts, lithofacies de Dunham, fabrique Turquie

1 - INTRODUCTION

Continental carbonate deposits have received significant attention over the last decade as they form important oil and gas reservoirs, mainly offshore Angola and in the South Atlantic (Volery *et al.*, 2010; Wright, 2012; Bahniuk *et al.*, 2015; Della Porta, 2015). In particular, travertines (Guo & Riding, 1992, 1994, 1998; Pentecost & Viles, 1994; Ford & Pedley, 1996; Pentecost, 2005) display fabrics that resemble those described within these South Atlantic reservoirs (Terra *et al.*, 2010; Rezende *et al.*, 2013; Ceraldi & Green, 2016; Saller *et al.*, 2016; Erthal *et al.*, 2017; Herlinger *et al.*, 2017). However, the studies on travertines have focused more on the distinction and the nomenclature of the travertine lithofacies (Pentecost, 2005; Capezzuoli *et al.*, 2014; Della Porta, 2015) as well as the description and classification of travertine and tufa lithofacies (Chafetz & Folk, 1984; Ford & Pedley, 1996; Guo & Riding, 1998; Arenas *et al.*, 2000; Özkul *et al.*, 2002, 2013; Arenas *et al.*, 2014; Gandin & Capezzuoli, 2014; Özkul *et al.*, 2014; Claes *et al.*, 2015; Orhan & Kalan, 2015; Croci *et al.*, 2016). Pre-Salt deposits of Lower Cretaceous Coqueiros and Macabu formations in Campos and Kwanza Basins, offshore Angola reflect hydrothermal alteration that might indicate existence of hydrothermal fluids percolating through faults (Herlinger *et al.*, 2017; Lima & De Ros, 2019; Lima *et al.*, 2020). These deposits hosting significant hydrocarbon reservoirs formed in environments where seismically discovered spring vents are present (Alvarenga *et al.*, 2016). Hydrothermal fluids that rose from these spring vents can be formed under subaqueous and subaerial conditions in a lacustrine environment (Claes *et al.*, 2015). As an analogue study to reservoir architecture of environments where hydrothermal circulation developed herein depositional processes of the Ballık travertines will be addressed by our integrated palaeoenvironmental approach including travertine quarry architectures which were associated with depositional environments.

2 - GEOLOGICAL SETTING

The Denizli Basin is a graben located in the western Anatolian extensional basin (Turkey). It is about 50 km long and 20 km wide (Koçyiğit, 2005; Westaway *et al.*, 2005; Kaymakçı, 2006; Alçiçek *et al.*, 2007; fig. 1). It hosts some of the most famous travertine bodies in the world (e.g. Pamukkale). The development of the latter is interpreted to be mainly tectonically controlled (Altunel & Hancock, 1993; Şimşek *et al.*, 2000; Kele *et al.*, 2011; Özkul *et al.*, 2013; Van Noten *et al.*, 2013, 2019). The travertine bodies at the northwest margin of the Denizli Basin mostly form in step-over zones between normal faults, whereas their counterparts located along its northwest and southeast sides are formed by thermal or cooler spring waters rising along normal faults and fractures (Altunel & Hancock, 1993; Şimşek *et al.*, 2000; Uysal *et al.*, 2007; Özkul *et al.*, 2013). Ballık travertine exposures located 5 km northwest of the Kaklık town, rest on Quaternary and Pliocene alluvial fans. The latter deposits overlie unconformably the Çökelez limestone of Jurassic to Cretaceous age. Within this study, six travertine quarries were studied in "Lower and Upper Domains" in the Ballık area, i.e. Faber-West, İllik, Best Abandoned and Demmer-Başaranlar at the Lower Domain, bounded by the Killik fault, which were already studied in terms of sedimentology, geochemistry and tectonic setting (Claes *et al.*, 2015; De Boever *et al.*, 2017; Van Noten *et al.*, 2019; Mohammadi *et al.*, 2020). These travertine quarries interfingered with Quaternary alluvial fans. In the Upper Domain, the studied Upper Tuna and Kömürcüoğlu travertine quarries, which are restricted by Düzçalı fault and a normal fault, are intercalated with Pliocene alluvial fans. The alluvial fan deposits lie upon these travertine quarries (fig. 1).

The geochemical signatures of travertines formed in Denizli-Horst Graben System (DHGS) have been used to unravel depositional conditions, and in some cases, related palaeoclimatic signals (Özkul *et al.*, 2010; Kele *et al.*, 2011; Toker *et al.*, 2015; Lopez *et al.*, 2017; Mohammadi

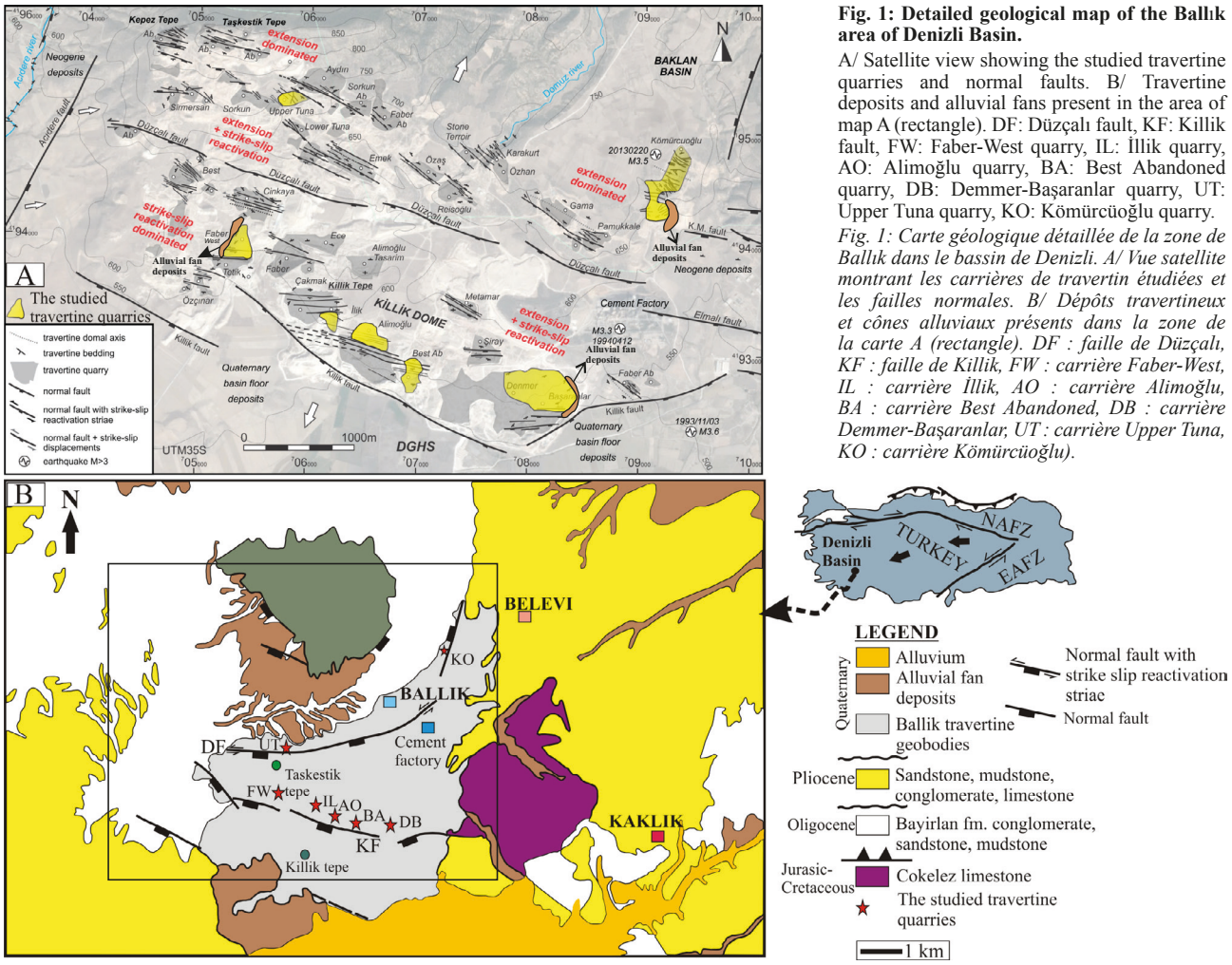

Fig. 1: Detailed geological map of the Ballık area of Denizli Basin.
A/ Satellite view showing the studied travertine quarries and normal faults. B/ Travertine deposits and alluvial fans present in the area of map A (rectangle). DF: Düzçalı fault, KF: Killik fault, FW: Faber-West quarry, IL: İllik quarry, AO: Alimoğlu quarry, BA: Best Abandoned quarry, DB: Demmer-Başaranlar quarry, UT: Upper Tuna quarry, KO: Kömürcüoğlu quarry.
Fig. 1: Carte géologique détaillée de la zone de Ballık dans le bassin de Denizli. A/ Vue satellite montrant les carrières de travertin étudiées et les failles normales. B/ Dépôts travertineux et cônes alluviaux présents dans la zone de la carte A (rectangle). DF : faille de Düzçalı, KF : faille de Killik, FW : carrière Faber-West, IL : carrière İllik, AO : carrière Alimoğlu, BA : carrière Best Abandoned, DB : carrière Demmer-Başaranlar, UT : carrière Upper Tuna, KO : carrière Kömürcüoğlu).

et al., 2020). Van Noten *et al.* (2013, 2019) described the tectonic evolution of the Lower and Upper Domain at the DHGS, bounded by the WNW-ESE oriented large-scale Killik and Düzçalı faults, respectively. The DHGS hosts more than forty travertine quarries which contain travertines that display high internal heterogeneity, including a complex organization. There has still been a deficit of detailed description of this sedimentological heterogeneity and therefore our study aims to reconstruct the depositional environments in the Lower and Upper Domains of the Ballık area by using lithofacies and sedimentary fabrics.

3 - MATERIALS AND METHODS

Sketches on photographs of the studied travertine quarries and lithologs from boreholes were made to deduce the depositional architecture. A map of the Ballık area was made using ArcMap software to document the topographic slope of the studied quarries. The palaeowater flow direction was deduced from different depositional geometries on the walls of Ballık travertine quarries. In all quarries, cores ranging between 2.54 and 10 cm in diameter were collected using a hand-held drilling machine to characterize individual lithofacies. In the Kömürcüoğlu travertine quarry, several boreholes were drilled behind several quarry walls and sedimentary logs reconstructed. Further boreholes from Demmer-Başaranlar quarry, drilled by the quarry owner, were also studied. The samples encompass the range of macroscopic sedimentological properties. The cores were plugged, and the plugs trimmed and impregnated twice with a fluorescent yellow-dye before thin-section preparation. The dye allows differentiating the outline of primary sedimentary fabrics as well as (micro)-porosity. Standard transmitted and polarizing light microscopy was performed using an Olympus BX60 and Leica DM LP Parallel and Crossed Polarizing Microscope (PPM and CPM, respectively) at KU Leuven (Belgium) and University of Manchester (UK). Scanning Electron Microscopy (SEM) analysis was carried out in the Sedimentology Department of Turkish Petroleum Corporation (TPAO) Research Company (Turkey).

4 - RESULTS

4.1 - NOMENCLATURE OF DUNHAM-BASED TRAVERTINE LITHOFACIES

Previous work has shown that integration of macroscopical properties of travertine lithofacies with their petrographical characteristics can be used to interpret depositional setting (Chafetz & Folk, 1984; Folk *et al.*, 1985; Guo & Riding, 1992, 1994; Jones & Renaut, 1995; Gandin & Capezzuoli, 2014;

Della Porta, 2015; Lopez *et al.*, 2017). Here, peloids, gastropods charophytes, phytoclasts, coated grains and intraclasts together with micrite matrix are primary components of packstone to grainstone, grainstone and wackestone lithofacies. The peloids form various fabrics such as pustular and irregular clotted fabrics, indicating reworked lime muds or micritic sediments which are often accompanied by broken gastropods and ostracods. Intraclasts are broken travertine clasts and frequently accompanied by peloids. Extraclasts, sometimes observed together with the intraclasts, refer to a broken particle of source rock composed of detrital quartz and clays. Packstone to grainstone texture has more peloids, coated grains, gastropods, charophytes than wackestone which has highly pores which result from decomposition of macrophytes and micritic or dendritic crusts. These macrophytes found as phytoclasts which consist of reworked liverworts, grasses, and reeds. On the one side, reed stems and bryophytes forming phytoherm are grown in situ. Dendrites branch upon these phytoherms, forming a crust. Besides, they can cover periphery of transported macrophytes and occur as coatings of coated grains which predominate packstone to grainstone lithofacies. In some cases, packstone to grainstone of coated grains interlayer with boundstone of stromatolites which contain undulatory-, flat- and columnar-laminated fabrics.

4.2 - DESCRIPTION AND CLASSIFICATION OF TRAVERTINE LITHOFACIES

Lithofacies were defined in hand-specimen according to (i) presence, volume and distribution of lime mud, (ii) presence and arrangement of dendrites, (iii) intraclasts and phyto mouldic pores, the latter related to phytoclasts and charophytes, (iv) coated grains , (v) skeletal remnants of gastropods or ostracods and (vi) extraclasts.

The travertines are described based on a modified Dunham (1962) classification. The detailed macroscopical characteristics of their lithofacies are presented in fig. 2. They consist of (i) packstone to grainstone (fig. 3A-3D), (ii) grainstone composed of coated grains (fig. 3E), (iii) wackestone of phytoclasts (fig. 3F-3H), (iv) boundstone of stromatolites (fig. 3I), v) crust of dendrites (fig. 3J), vi) phytoherm of reeds (fig. 3K) and bryophytes (fig. 3L).

4.2.1 - Packstone to grainstone

Description

The matrix of this lithofacies usually has a massive micrite fabric that is characterized by a distribution of patchy anhedral micrites (crystal size: < 4 μm; fig. 4A), whereas the grain composition consists mainly of intraclasts, extraclasts, coated grains that constitute 30 % of total grains and charophytes, gastropods or ostracods which have a relative abundance of 20 % (fig. 4B-C). The extraclasts are composed of detrital and clay particles with detrital illite and minor kaolinite (fig. 4D). The coated grains are characterized by different textures in terms of composition. The first consists of elongate fibres, about 0.4 mm in diameter with blunt terminations oriented parallel or parallel to their c-axis, growing radially outward from a small hole (fig. 4E-F). The second one comprises numerous, ~1 mm thick, knob-like peloidal nuclei (fig. 5A) that are 0.2 to 0.3 mm in diameter and coatings with 0.2 mm thick irregular wavy sparry laminations (fig. 5B). Sometimes, these peloids of about 0.6 mm in diameter are surrounded by radially arranged dendrite micrites which range between 1 and 1.5 mm in length (fig. 5C). Each dendrite exhibits undulatory extinction under cross polarized light. In some cases, these dendrites are less tightly packed and composed of elongated sparite crystals (fig. 5D).

These grains make up a wavy lamination (fig. 3B), along with abundant intraclasts. The intraclasts are characterized by irregular clotted fabric comprising a complex amalgamation of rounded to elongated peloids forming irregular clotted fabric. They are accompanied by extraclasts along with a minor amount of broken ostracod and gastropod shells (fig. 6A, B). The clotted fabric contains a network of 10 μm thick and elongated micritic filaments, which separates pores filled by calcite microspar (fig. 6C). Local bioturbation occurs in association with V-shaped vuggy pores with a basal fill of dendrites which branch into the pore (fig. 6D).

Interpretation

Microfacies properties of this lithofacies reflect clearly environmental conditions. Moderately flowing water could have washed out the lithofacies-building rock constituents broken from a proximal or distal slope environments (e.g. De Boever *et al.*, 2017) towards a marsh pool environment (Guo & Riding, 1998), resulting in a mixture of intraclasts, coated grains, broken gastropod shells, and extraclasts which should be the product of alluvial fans. Their heterogeneity can result from physical reworking of grains due to short-lived pluvial events (Wright & Barnett, 2015). Intraclasts could represent the stems of phreatophytic plants (Semeniuk & Meagher, 1981) and calcified root-stems (Klappa, 1978) which penetrate into micritic matrix under palustrine conditions developed within a pool environment (Alonso & Wright, 2010).

Changes in flow energy, ionic strength and supersaturation of fluids and microbial activity enabled coated grains with various composition to be formed in different environmental conditions. The coated grains with radial fibres can occur as thin laminae in shallow waters (Rossi & Cañaveras, 1999). The preservation of fibres, within which black-stained microbial imprints could be developed, might indicate oxidized meteoric water (Rossi & Cañaveras, 1999). On the one hand, Lippman (1973) suggested that their origin should be attributed to abiotic processes in relation to progressive desiccation and/or supersaturation of the water. Sometimes, packstone to grainstone of coated grains, which have peloidal nuclei and coatings of dendrites and sparry laminae, occurred as small mound heads that developed in gently dipping slopes (De Boever *et al.*, 2017; Erthal *et al.*, 2017) and in flood plain environment. This type can be attributed to agitated or faster flowing water through which high CO_2 degassing gives a crystalline appearance to micritic

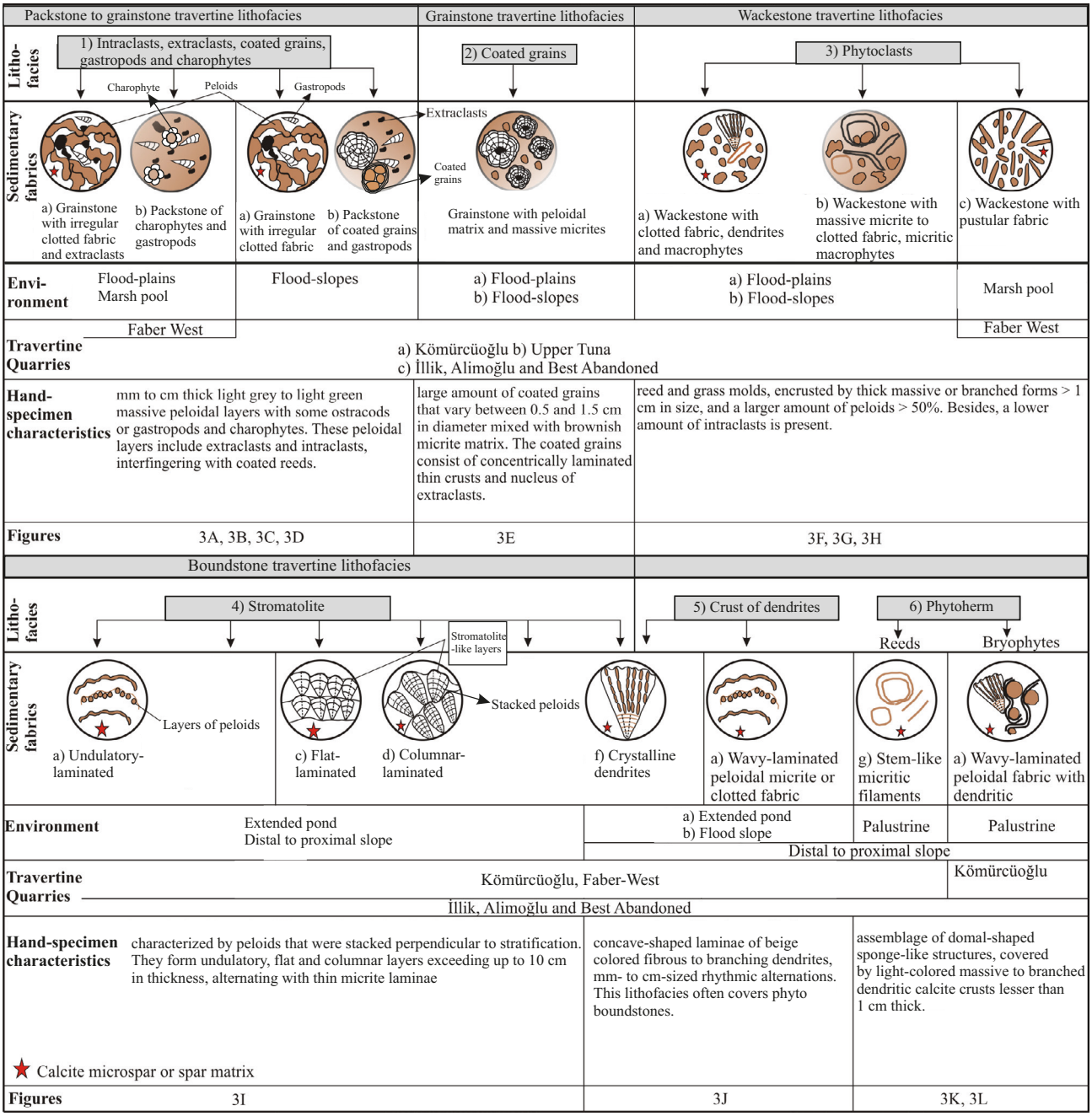

Fig. 2: Hand-specimen characteristics integrated with schematized sedimentary fabrics of packstone to grainstone, grainstone of coated grains, wackestone of phytoclasts, boundstone of stromatolites, crust of dendrites, phytoherm of reeds and grasses travertine lithofacies.

Fig. 2: Caractéristiques des échantillons intégrées avec les schémas des fabriques sédimentaires des lithofaciès de travertin de types packstone à grainstone, grainstone à grains enrobés, wackestone de phytoclastes, boundstone de stromatolites, croûte de dendrites, phytoherme de roseaux et herbes.

dendrites in a slope environment (Chafetz & Guidry, 1999; Erthal *et al.*, 2017). In contrast, Pedley (1990) proposed that slow water flow could give rise to this type of coated grains, referred to as oncoidal peloids (Folk & Chafetz, 1983; Chafetz & Folk, 1984).

4.2.2 - Grainstone of coated grains lithofacies

Description

Coated grains forming grainstone texture have irregularly dispersed nuclei composed of extraclasts and peloids which are characterized by different coatings. The extraclasts are asymmetrically or symmetrically coated by thin micrite laminae of 0.5 mm in thickness in a granular matrix (fig. 7A). On the one hand, coatings on peloids consist of radially arranged fan-shaped calcites. The granular matrix is composed of peloids with a diameter varying around 50 µm (fig. 7B), exhibiting very strong undulose extinction under cross polarized light (fig. 7B).

Interpretation

This lithofacies resembles radial shrub pisoids, in terms of the size of coated grains and undulose extinction of fan-shaped calcites forming coatings, which are interpreted to form in agitated pools and lenticular-shaped depressions (Chafetz & Folk, 1984; Guo & Riding, 1994; Croci *et al.*, 2016). In this sense, peloids and extraclasts forming a nucleus of the coated grains were reworked in calcium bicarbonate saturated waters, where agitated waters enabled the peloids and extraclasts to be coated by fan-shaped calcites.

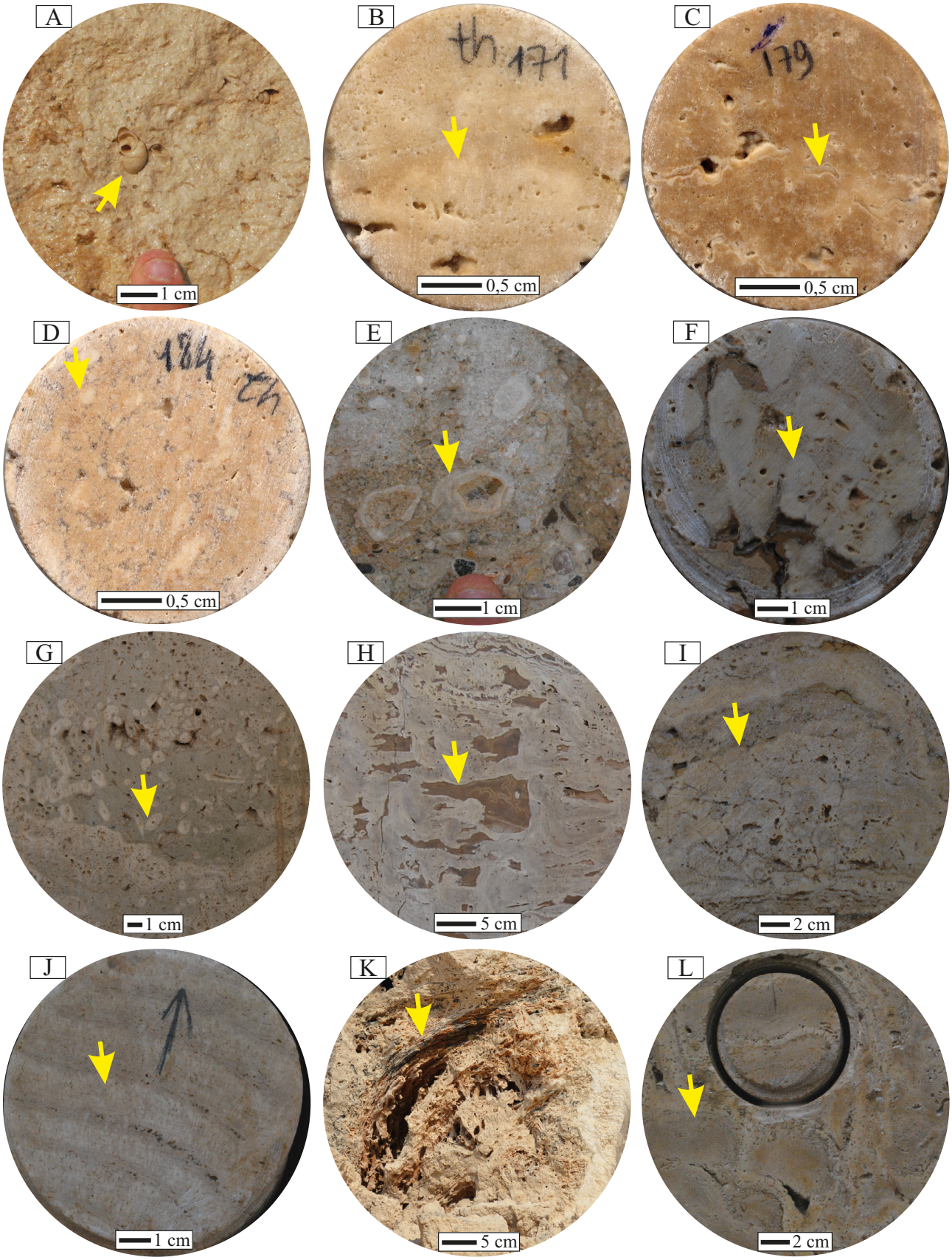

Fig. 3: Pictures of hand-specimen characteristics of packstone to grainstone (PG), grainstone of coated grains, wackestone of phytoclasts, boundstone of stromatolites, crust of dendrites, phytoherm of reeds and grasses lithofacies observed in the Ballık area.

Yellow arrows indicate (A) a gastropod shell in PG lithofacies, (B) a layer of coated grains in PG lithofacies, (C) traces of bioturbation in PG lithofacies, (D) intraclasts of PG lithofacies, (E) a grainstone of coated grains, (F and G) wackestones of phytoclasts, (H) cemented vugs formed within wackestone of phytoclasts, (I) a boundstone of coated grains, (J) a crust of dendrites, (K) a phytoherm of reeds and (L) a phytoherm of bryophytes.

Fig. 3: Photographies des échantillons caractéristiques des lithofaciès packstone à grainstone (PG), grainstone à grains enrobés, wackestone de phytoclastes, boundstone de stromatolites, croûte de dendrites, phytoherme de roseaux et herbacées observés dans la zone de Ballık. Les flèches jaunes indiquent (A) une coquille de gastéropode dans le lithofaciès PG, (B) une couche d'intraclastes dans le lithofaciès PG, (C) des traces de bioturbations dans le lithofaciès PG, (D) des intraclasts du lithofaciès PG, (E) un grainstone de grains enrobés, (F et G) des wackestones de phytoclastes, (H) des vacuoles cimentées formées dans des wackestones de phytoclastes, (I) un boundstone de grains enrobés, (J) une croûte de dentrites, (K) un phytoherm de roseaux, (L) un phytoherm de bryophytes.

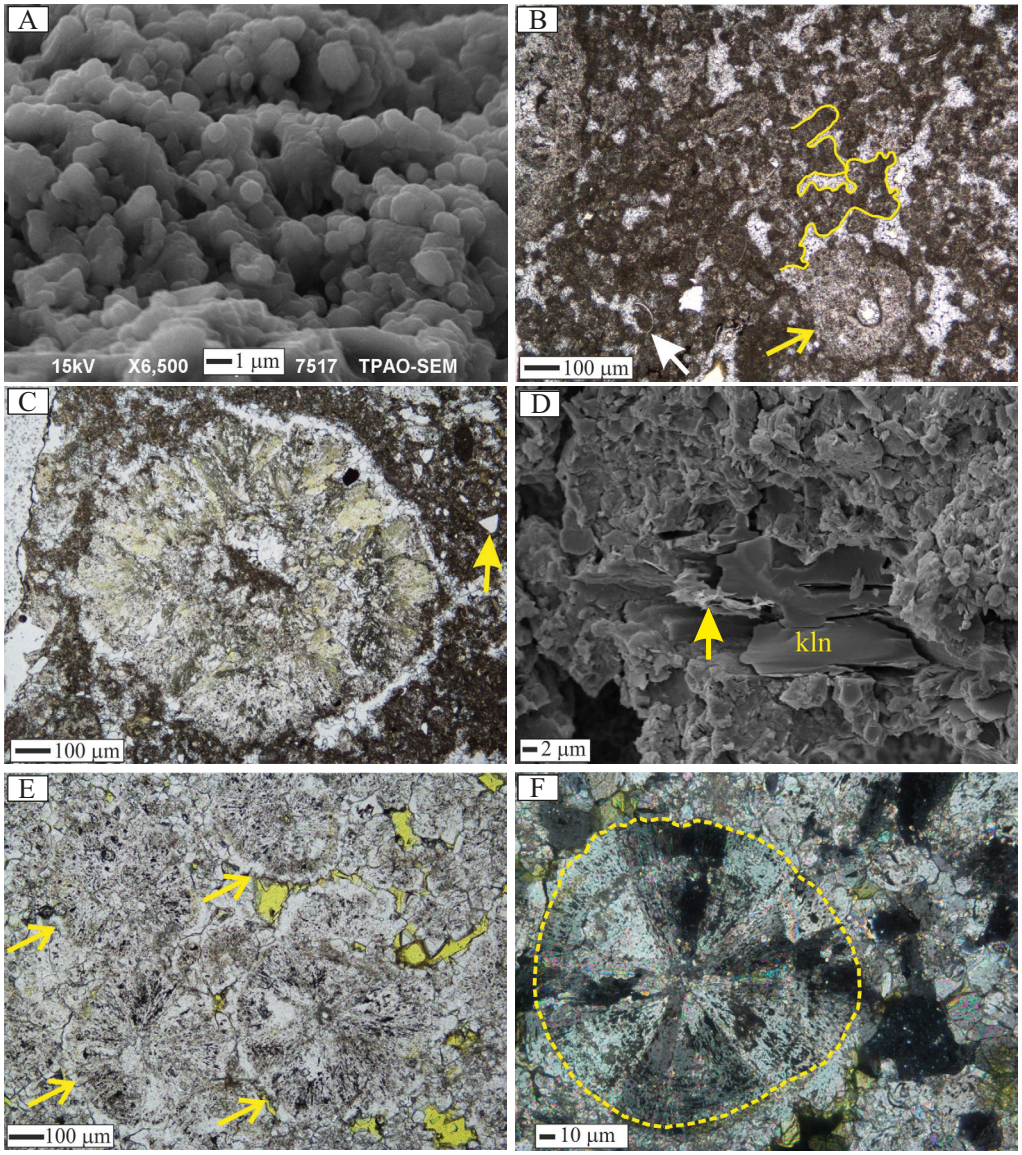

Fig. 4: Pictures of packstone to grainstone lithofacies.
A/ Massive micritic matrix (SEM image). B/ Irregular clotted fabric (yellow line) with broken chara (yellow arrow) and disarticulated ostracod shells (white arrow). C/ Intraclast and a few quartz particles (yellow arrow). D/ Kaolinite (kln) and illite (yellow arrow) clay particles (SEM image). E/ Coated grains with radial fibres (yellow arrows). F/ Close-up image of a coated grain (yellow dotted circle) from E under crossed polarized light.

Fig. 4 : Photographies au MEB de lithofaciès packstone à grainstones. A/ Matrice micritique massive. B/ Fabrique irrégulière avec des charas cassées (flèche jaune) et des coquilles d'ostracodes (flèche blanche). C/ Intraclaste et quelques particules de quartz (flèche jaune). D/ Particules argileuses : kaolinite (kln) et illite (flèche jaune) (SEM). E/ Grains enrobés avec une structure radiale fibreuse (flèches jaunes). F/ Zoom sur un grain enrobé (cerle jaune pointillé) de l'image E en lumière polarisée croisée.

4.2.3 - Wackestone of phytoclasts lithofacies

Description

Wackestone of phytoclasts consists of fragments of elongated to V-shaped macrophytes that are smaller than 1 mm in size (fig. 7C-D). These fragments are coated by a high abundance of micrite (fig. 7C) and peloids forming a clotted fabric (fig. 7D), indicating remnants of liverworts. Some are surrounded by tightly-packed dendrites (fig. 7E-F). Moss-like stems with a meshwork of micritic filaments are observed together with clotted fabrics (fig. 7G). Pustular fabrics are built by clumped peloids that range from 0.5 to 1 mm in diameter (fig. 7H) and develop around sub-spherical to rounded-shaped pores that are larger than 1 mm in size. These large pores refer to the elongate sections of decomposed plant fragments, considerably surrounded by light-coloured lime muds in outcrop. Isopach and blocky calcite spars are preferentially formed around pustular and clotted fabrics as well as micrite filaments and occur as cements in the wackestone texture.

Interpretation

Fragments of macrophytes are encrusted during transportation and accumulate within pool environment (Ford & Pedley, 1996; Guo & Riding, 1998; Claes *et al.*, 2015; Lopez *et al.*, 2017; fig. 3F-G). The lithifications of liverworts with open V-shaped structure (fig. 7C) and moss-like stems (fig. 7G) can give rise to small obstacles, which inhibit water flow, in pools and besides have been observed in palustrine conditions (Arenas *et al.*, 2000; Pentecost, 2005; Arenas *et al.*, 2007). Generally, organic parts of macrophytes are decomposed. The resulting pores are surrounded by tightly-packed dendrites and peloids. Moreover, pustular fabrics and micrite filaments represent extracellular coatings developed along branches of macrophytes as explained in figure 2 (Anadon *et al.*, 2000). Calcite spar cements likely resulting from the infiltration of near-surface meteoric waters readily fill up the main stem-molds of decayed plants (Saller *et al.*, 1994; Lønøy, 2006).

4.2.4 - Boundstone of stromatolites

Description

Boundstone of stromatolites which are made of wavy-, columnar- and flat-laminated fabrics are found to be intercalated with packstone to grainstone of coated grains. The undulatory-laminated fabric composed of well-rounded peloids ranging from 50 to 100 µm

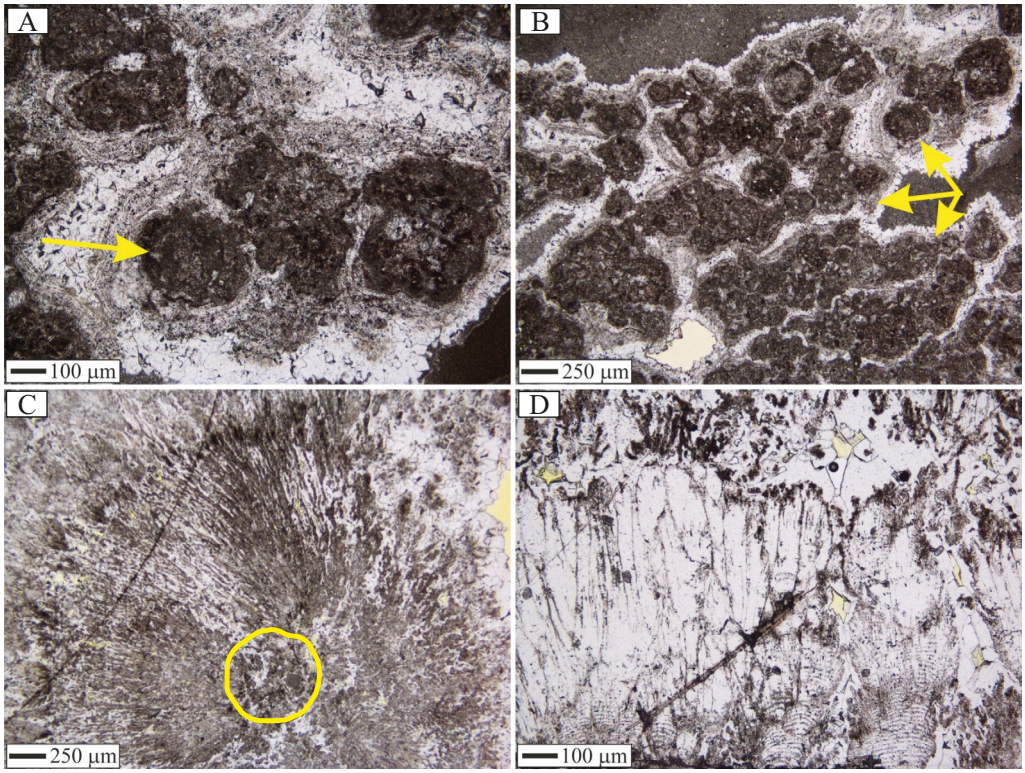

Fig. 5: Packstone to grainstone of coated grains lithofacies.

A/ Concentrically calcite-coated peloids (yellow arrow). B/ Coated grains with peloidal nuclei and coating of sparry laminae (yellow arrows). C/ Coated grain having coatings of dendrites (yellow circle). D/ Tightly-packed crystalline dendrites.

Fig. 5 : Lithofaciès packstone à grainstones de grains enrobés. A/ Péloïdes à couches d'enrobage concentriques de calcite (flèche jaune). B/ Grains enrobés avec un noyau peloidal et un revêtement de lamines sparitiques (flèches jaunes). C/ Grains enrobés recouverts de dendrites (cercle jaune). D/ Dendrites cristallines très serrées.

in diameter, displaying concave to convex-shaped alignments surrounded by blocky sparites (fig. 8A). The columnar-laminated fabric comprised of stacked peloids with a length to width ratio (LWR) larger than 1 (fig. 8B). The flat-laminated fabric with fan-shaped calcites having a LWR lower than 1 is tightly aligned, displaying wavy laminations (fig. 8C-D). The flat-laminated fabric also shows stronger undulatory extinction than undulatory- and columnar-laminated fabrics.

Interpretation

The columnar- and flat-laminated fabrics should represent rims of mound heads (fig. 3I) lithified by calcium bicarbonate-rich fluids (Claes *et al.*, 2015; Mohammadi *et al.*, 2020) along these slopes. On the one hand, undulatory-laminated fabric can be related to more stagnant or slow flowing water, likely providing low energy conditions in the extended pond or pool environments (Pentecost, 2005).

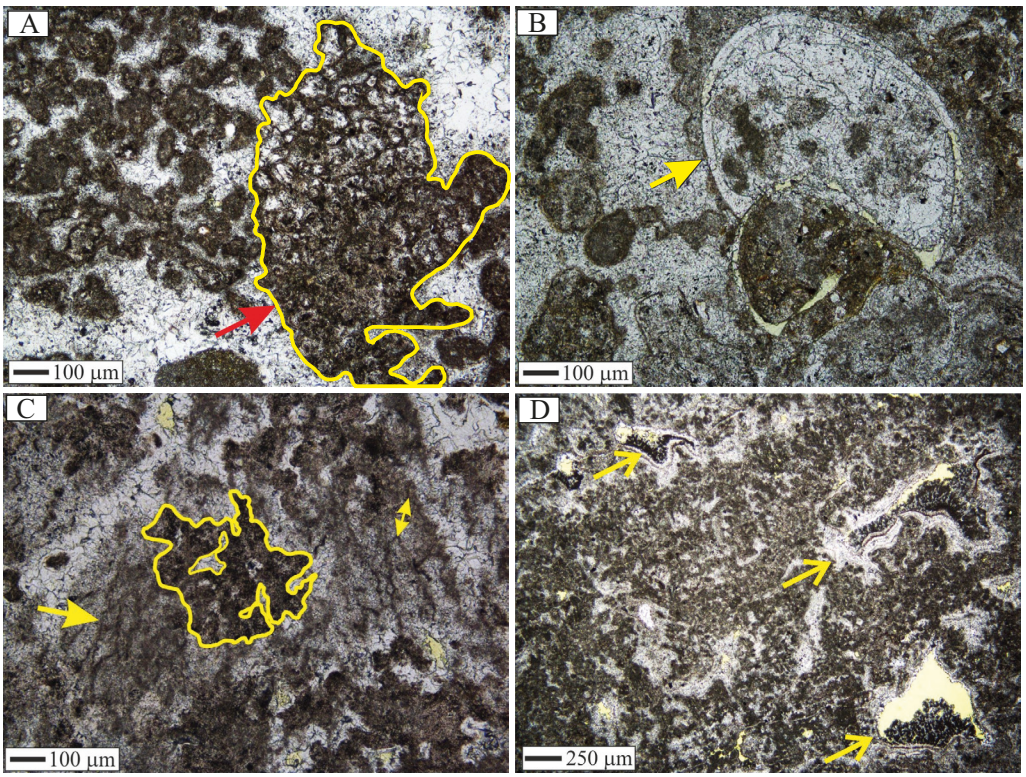

Fig. 6: Packstone to grainstone (PG) lithofacies.

A/ Sparitic extraclasts (red arrow and yellow line) within irregular clotted fabric. B/ Gastropod shell (yellow arrow). C/ Network of micritic filaments (yellow arrows) highlighted by pores next to an irregular clotted fabric (yellow line). D/ Branches of micritic filaments with vuggy pores (yellow arrows).

Fig. 6: Lithofaciès packstone à grainstone (PG). A/ Extraclastes sparitiques (flèche rouge et ligne jaune) dans une fabrique coalescente irrégulière. B/ Coquille de gastéropode (flèche jaune). C/ Réseau de filaments micritiques (flèches jaunes) mis en évidence par des pores à côté d'une fabrique coalescente irrégulière (ligne jaune). D/ Branches de filaments micritiques avec des pores vacuolaires (flèches jaunes).

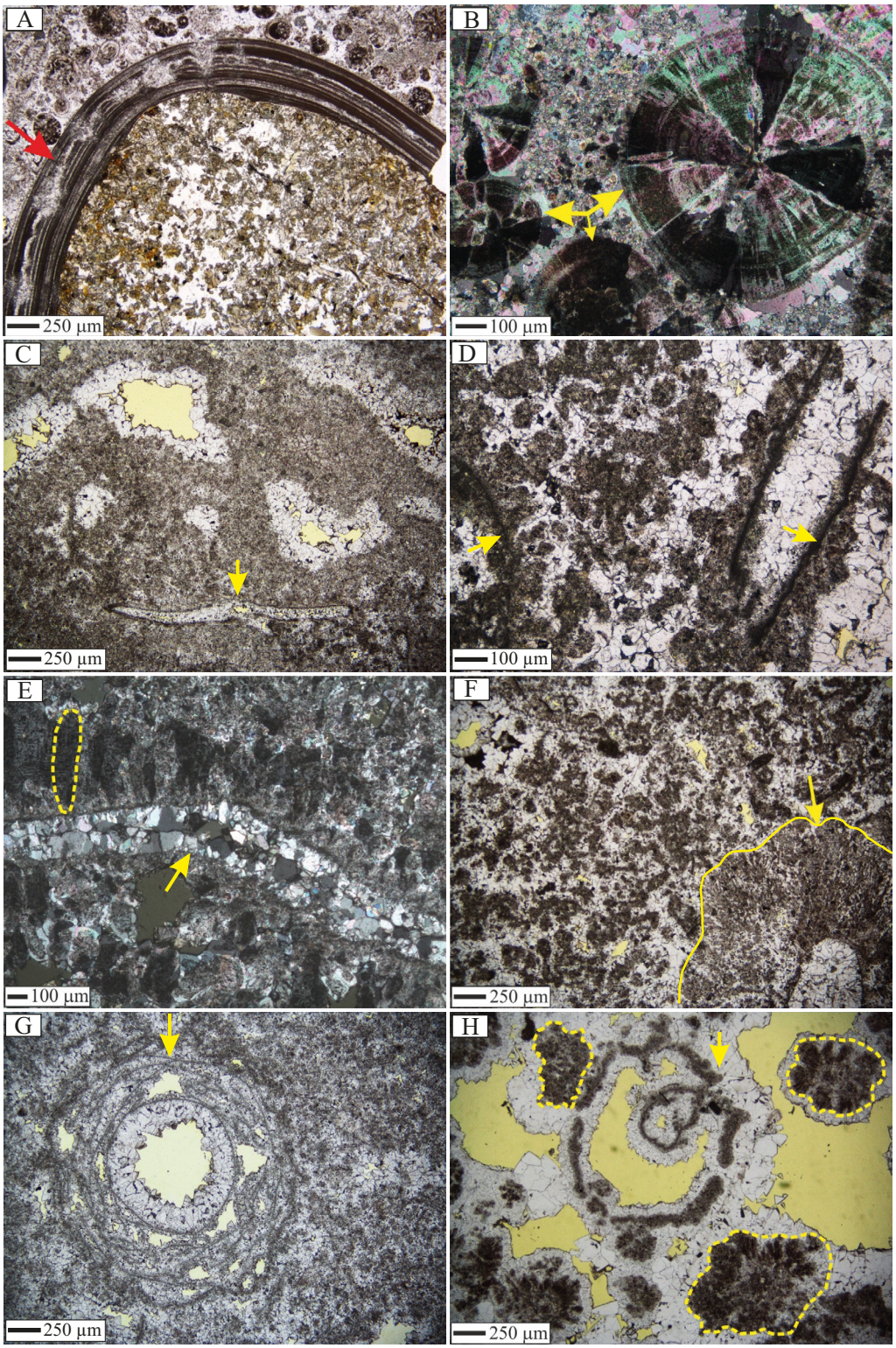

Fig. 7: Grainstone of coated grains (A, B) and wackestone of phytoclasts (C to H).

A/ Micrite coatings (red arrow) surrounding an extraclast in the grainstone. B/ Coated grains with coatings of fan-shaped calcite crystals (yellow arrows) forming the grainstone. C/ V-shaped macrophyte (yellow arrow) within massive micritic matrix of the wackestone. D/ Elongated, micritic reed stems surrounded by clotted fabric in the wackestone. E/ Peloids (yellow dotted line) next to V-shaped macrophyte (yellow arrow) in the wackestone. F/ Clotted fabric including tightly-packed dendrites (yellow arrow) developed upon an elongated reed stem in the wackestone. G/ Moss-like stems (yellow arrow) within clotted fabric of the wackestone. H/ Pustular fabric (yellow circle) in the wackestone.

Fig. 7 : Grainstones (A et B) et wackestone de phytoclastes (C à H). A/ Revêtements micritiques (flèche rouge) entourant un extraclaste dans le grainstone. B/ Grains enrobés à revêtement de cristaux de calcite en éventail (flèches jaunes) formant le grainstone. C/ Macrophyte en forme de V (flèche jaune) dans la matrice massive micritique du wackestone. D/ Tiges de roseau micritiques allongées entourées d'une fabrique grumeleuse dans le wackestone. E/ Péloïdes (ligne pointillée jaune) à côté d'un macrophyte en forme de V (flèche jaune) dans le wackestone. F/ Fabrique grumeleuse comprenant des dendrites très serrées (flèche jaune) développées sur une tige de roseau allongée dans le wackestone. G/ Tiges en forme de mousse (flèche jaune) dans la fabrique grumeleuse du wackestone. H/ Fabrique pustuleuse (cercle jaune) dans le wackestone.

4.2.5 - Crust of dendrites

Description

It consists of dendritic layers intercalated with brown-coloured layer (fig. 3J). The dendrites having at most 1 cm thickness exhibit tightly-packed crystalline branches with very strong undulose extinction (fig. 9A-B) whereas the brown-coloured layer is characterized by intercalations of thin, wavy-laminae composed of peloids with a length of about 1 mm. These peloids often develop on the crystal terminations of these zig-zag shaped crystalline dendrites and form a clotted fabric, being rimmed by isopach sparite (fig. 9A).

Interpretation

Crust of dendrites lithofacies is found as rimstone barriers occurred in pool environment (Jones & Renaut, 1995). Tightly-packed dendrites are likely formed by fast precipitation and increasing CO_2 degassing under faster flowing waters with turbulence (Zhang *et al.*, 2001; Chen *et al.*, 2004; Jones *et al.*, 2005). Peloidal laminae that inhibit growth of these dendrites likely result from seasonal changes (Pentecost, 2005; Erthal *et al.*, 2017).

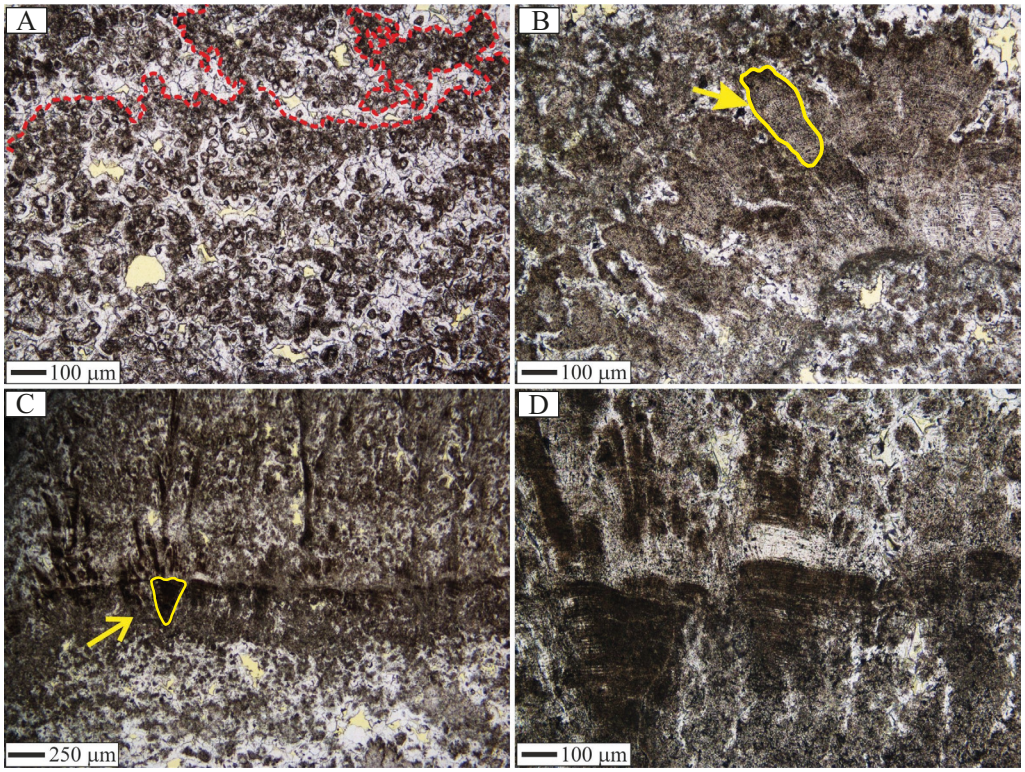

Fig. 8: Boundstone of stromatolites lithofacies.
A/ Wavy-laminated fabric (dotted red line). B/ Columnar-laminated fabric (yellow arrow). C/ Fan-shaped calcites (yellow arrow) forming flat-laminated fabric. D/ Close-up of flat-laminated fabric from image C.
Fig. 8 : Lithofaciès boundstone de stromatolithes. A/ Fabrique laminée ondulée (ligne rouge pointillée). B/ Fabrique laminée en colonnes (flèche jaune). C/ Calcites en éventail (flèche jaune) formant une fabrique laminée plate. D/ Zoom sur la fabrique laminée plate de l'image C.

4.2.6 - Phytoherm of reeds and bryophytes

Description

Phytoherm lithofacies has two textures. Organic parts of phytoherm with reeds are decayed and their crusts are left while phytoherm of bryophytes is partially preserved. The phytoherm of reeds comprises an integrated fabric of micrite filaments and dendrites as well as massive sparite fabric (fig. 9C-D), whereas the one with bryophytes is made up by wavy-laminated peloidal fabrics (fig. 9E). The first lithofacies has a spongy fabric due to the high abundance of moldic porosity that is associated with inner empty stem-like features. These features are typically larger than 1 mm in diameter aligned by subparallel concentric micritic filaments with ring-shaped outline that are 0.05 to 0.1 mm in diameter (fig. 9C). The outer micritic crust around these stem-like forms is surrounded by tightly-packed dendrites that are about 1 mm in size. The tiny crust consists of peloids up to 0.2 mm in diameter which is commonly covered by isopachous calcite spar, approximately 0.06 to 0.1 mm in size. Massive sparite fabrics (fig. 9D) are observed where these micritic stem-like forms predominate. The wavy-laminated peloidal fabric of phytoherm with bryophytes is mainly comprised of wavy-laminated discrete and rounded peloids (fig. 9E-F) that are 0.1 to 0.2 mm in size, which are covered by tightly-packed crystalline dendrites (fig. 9G-H). This fabric can act as a substrate for the development of large sparite crystals.

Interpretation

Macrophytes or microphytes grow *in situ* in varying directions with respect to the underlying substrate and the flowing water. Crusts cover sponge-like small dams formed under palustrine conditions (Ford & Pedley, 1996; Guo & Riding, 1998; Arenas *et al.*, 2000, 2007; Claes *et al.*, 2015). The physical fabric of such dams differs from small mounds of calcite-coated plants in different environment conditions (Pentecost, 2005). Plant diversity appears to be high in the phytoherm. The bryophytes forming phytoherm are likely indicative of acrocarpous moss (Pentecost & Zhaohui, 2002), reflecting moss stems from hygrophytic plants (Arenas *et al.*, 2007). These plants are known to densely colonize under very low water flow conditions. Their stems provide enough suitable surface area to be encrusted by calcium carbonate (Pentecost & Zhaohui, 2002) generating massive sparite fabrics including dispersed micrites. The phytoherm of bryophytes possesses thicker crusts characterized by wavy-laminated clotted fabrics that are surrounded by tightly-packed dendrites. Because bryophytes compared to reeds have larger surface area, higher evaporation and CO_2 degassing (Pentecost, 2005). Besides phytotherm of bryophytes is occurred under thicker water laminae.

4.3 - DEPOSITIONAL ENVIRONMENTS OF TRAVERTINE QUARRIES IN THE BALLIK AREA

The Ballık area in Denizli Horst-Graben System (DHGS) hosts several well-excavated Quaternary travertine quarries, occurring in a "Lower and Upper Domain". After travertine precipitation, tectonic uplift occurred along graben shoulders, causing the separation between the "Lower Domain" and the "Upper Domain". These domains were defined by the large-scale Killik and Düzçalı faults (Van Noten *et al.*, 2019). This uplift caused significantly variations in discharge and flow velocity of spring waters and besides different local spring locations which control the morphology and internal stratification of a travertine deposits (Chafetz & Folk, 1984; Guo & Riding, 1998; Goldenfeld *et al.*, 2006; Della Porta, 2015).

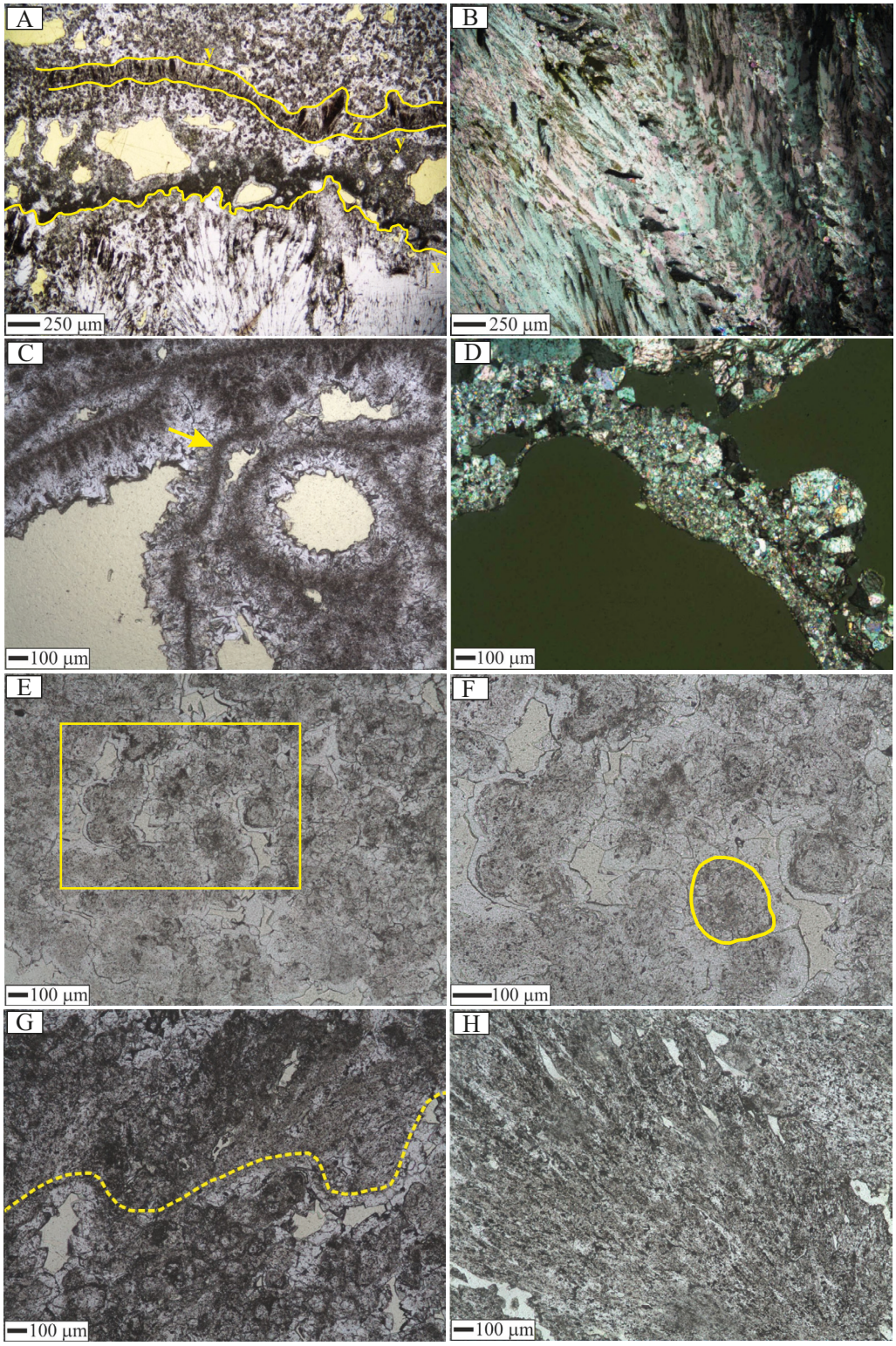

Fig. 9: Crust of dendrites (A, B) and phytoherm of reeds and bryophytes (C to H) travertine lithofacies.

A/ Alternating tightly-packed crystalline dendrite fabric (x), wavy-laminated peloidal fabric (y), and loosely-packed dendrite fabric (z) across lamination (each laminae separated by a yellow line). B/ Tightly-packed crystalline dendrite fabric. C/ Fabric of ring-shaped micrite filaments (yellow arrow) and dendrites. D/ Massive sparite fabric. E/ Wavy-laminated peloidal fabric (the yellow rectangle indicates the contours of image F). F/ Close-up image of a peloid from image E (yellow circle). G/ Distinction between wavy-laminated peloidal fabric and tightly-packed crystalline dendrite fabric (dotted yellow line). H/ Close-up image of tightly-packed crystalline dendrite fabric.

Fig. 9 : Lithofaciès de travertin à croûtes de dendrites (A, B) et à phytoherme de roseaux et bryophytes (C à H). A/ Alternance d'une fabrique dendritique cristalline très serrée (x), d'une fabrique péloïdale ondulée (y) et d'une fabrique dendritique cristalline lâche (z) le long de la stratification (chaque lamine est séparée par une ligne jaune). B/ Fabrique dendritique cristalline très serrée. C/ Fabrique de filaments de micrite de forme circulaire (flèche jaune) et de dendrites. D/ Fabrique de sparite massive. E/ Structure péloïdale ondulée (le rectangle jaune indique les contours de l'image F). F/ Zoom sur un péloïde de l'image E (cercle jaune). G/ Distinction entre la fabrique peloïdale laminée onduleuse et la fabrique dendritique cristalline très serrée (ligne jaune pointillée). H/ Détail de la fabrique dendritique cristalline très serrée.

The travertine quarry architecture is described according to vertical transitions between different depositional environments which are mainly structured by the type and abundance of travertine lithofacies (Chafetz & Folk, 1984; De Boever *et al.*, 2017; Lopez *et al.*, 2017). Lithofacies-based lithologs and sketches, presented in this study, allowed determination of environmental changes and construction of a conceptual depositional model for the (i) Faber-West, Demmer-Başaranlar, İllik, Alimoğlu, Best-Abandoned and (ii) Upper-Tuna, Kömürcüoğlu quarries from Lower Domain and Upper Domain, respectively.

4.3.1 - Depositional environment of travertine quarries at the Lower Domain

4.3.1.1 - İllik, Alimoğlu and Best Abandoned travertine quarries

Description

İllik quarry comprises mainly a mixture of packstone to grainstone of intraclasts, wackestone of phytoclasts and less amount of boundstone of stromatolites. Phytoherm of reeds are highly interfingered with wackestone of phytoclasts lithofacies. The latter lithofacies and packstone to grainstone form marsh pool environment while palustrine environment is characterized by high

amount of phytoherm of reeds lithofacies. Boundstone of stromatolites lithofacies form in extended pond and proximal to distal slope environment with smooth to microterrace layers which evolve upward into crinkly to disturbed layers of marsh pool environment integrated with palustrine deposits (fig. 10). The extended pond and proximal to distal environments display clear stratification of slightly (< 2°) dipping layers. The proximal to distal slope environment displays downstream changing lithofacies geometries, respectively as follows: (i) alternating phytoherm of bryophytes and crust of dendrites lithofacies having continuous smooth to microterraces layers, (ii) phytoherm of reeds covered by crust of dendrites lithofacies, characterized by anisopachous and discontinuous steep layers.

Alimoğlu quarry consists of packstone to grainstone of intraclasts which is overlain by a large amount of wackestone of phytoclasts. The phytoherm of reeds lithofacies cover these lithofacies, which give rise to 15 m thick marsh pool environment, forming a palustrine environment (fig. 10).

The extended pond environment in the İllik quarry has not been observed in the southeastern part of Alimoğlu quarry because phytoherm of reeds is observed to be extended increasingly towards the Alimoğlu travertine quarry (fig. 10). Water flow direction in the İllik travertine quarry is very consistent with that of the Best Abandoned and Alimoğlu quarries, which formed a few hundred meters further towards the east (fig. 11A-B). The Best Abandoned quarry has highly fractured zone with

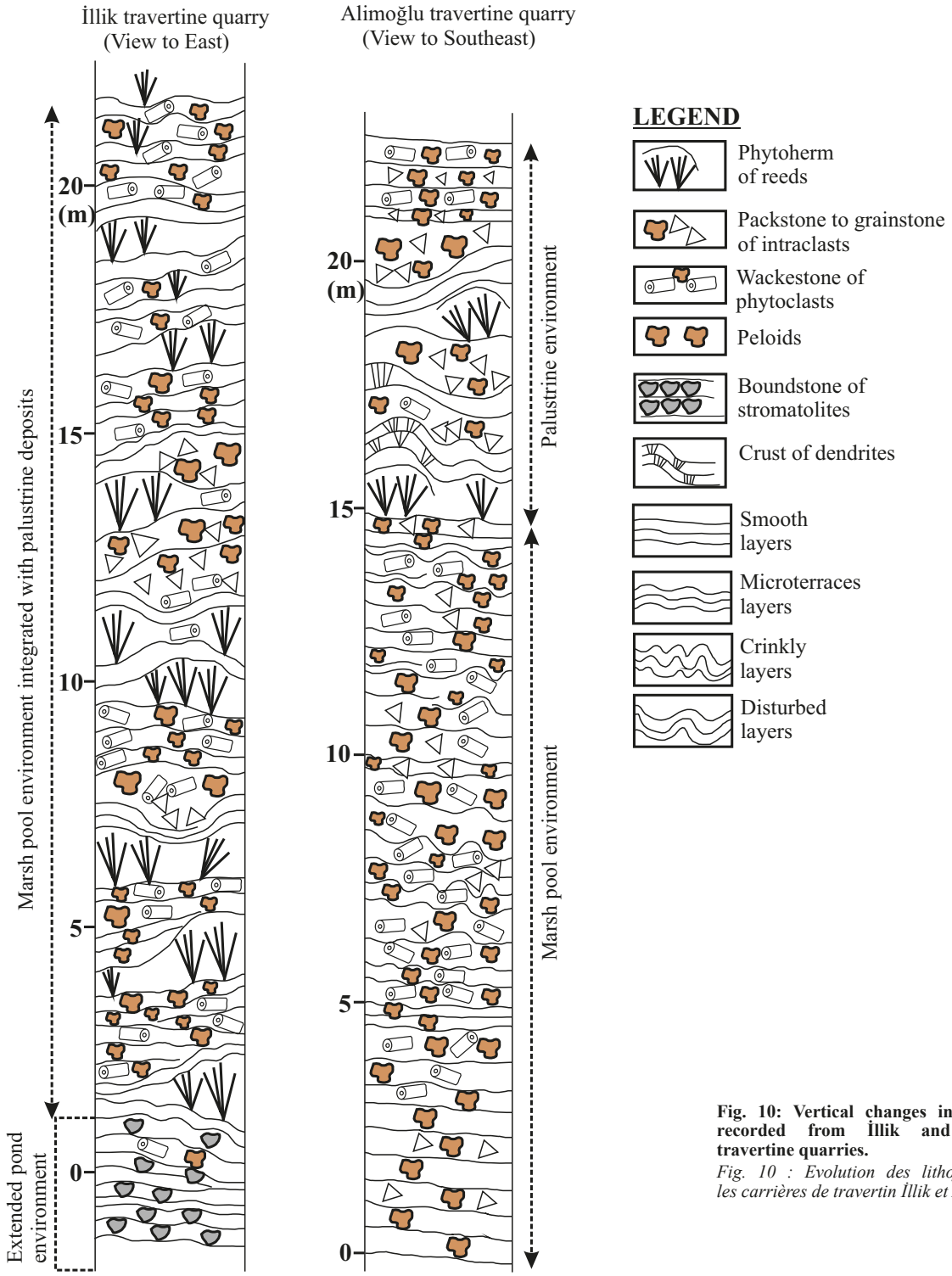

Fig. 10: Vertical changes in lithofacies recorded from İllik and Alimoğlu travertine quarries.

Fig. 10 : Evolution des lithofaciès dans les carrières de travertin İllik et Alimoğlu.

smooth to microterraced layers dipping to the north side and with smooth layers to the south. This zone consists of intraclast-rich packstone to grainstone with irregular clotted fabric and wackestone of phytoclasts which also form as fracture in-fills (fig. 11C).

Interpretation

These quarries located in the eastern part of the "Lower Domain" were properly delineated in terms of lithofacies properties (Swennen *et al.*, 2017; Claes *et al.*, 2019). However, they have not yet been worked out based on travertine environments by considering lithofacies-based lithologs and sketches which refer to a formation of "steepening up" depositional architecture (Guo & Riding, 1998). The latter indicates that extended pond environment evolved into marsh pools in which phytoherm of reeds forms in palustrine conditions. This evolution of environments was previously also determined in Çakmak quarry, which occurs westward of the above mentioned quarries in the "Lower Domain" (De Boever *et al.*, 2017; Mohammadi *et al.*, 2020). Presence of boundstone of stromatolites is a very typical aspect for the extended pond environment. Similarly, these deposits were described as shrubs which, in some cases, form rims of proximal to distal slope environments (Chafetz & Folk, 1984; De Boever *et al.*, 2017; Mohammadi *et al.*, 2020). The proximal and distal slopes are dipping in WNW direction in the Çakmak quarry (De Boever *et al.*, 2017), while they dip to the north and west in Faber quarry, to the southeast and northwest sides in

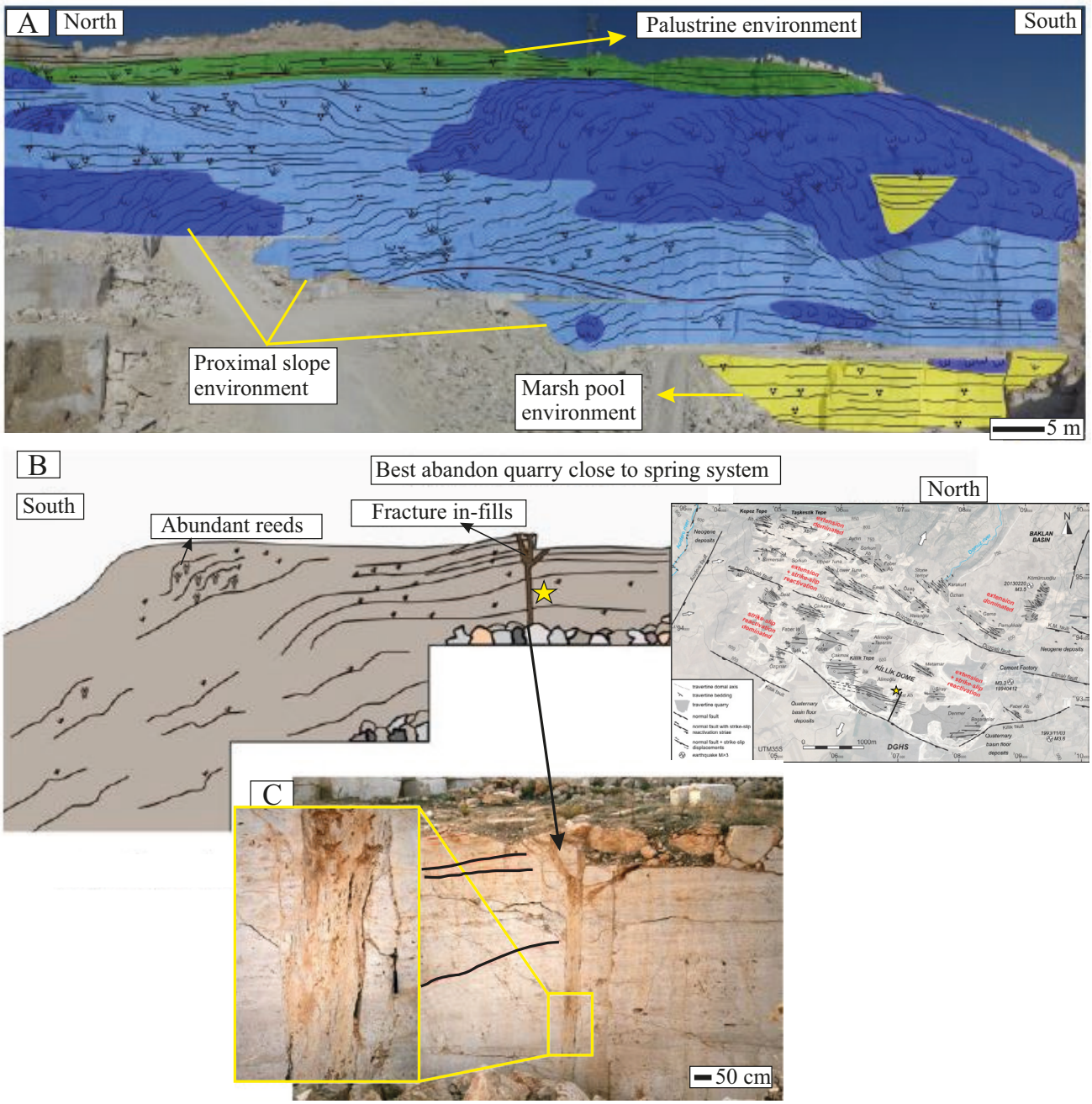

Fig. 11: Depositional environments formed in the İllik and Best Abandoned travertine quarries.
A/ Depositional architecture of İllik travertine quarry. B/ Damage zone at the Best Abandoned quarry where a spring system was recognised (yellow star). C/ Fracture infillings in spring feeder system where the packstone to grainstone and wackestone lithofacies formed.
Fig. 11 : Environnements sédimentaires formés dans les carrières de travertin İllik et Best Abandoned. A/ Architecture sédimentaire de la carrière de travertin İllik. B/ Zone de dommages dans la carrière Best Abandoned où un système de sources a été reconnu (étoile jaune). C/ Remplissage de fracture dans le système d'alimentation de la source où les lithofaciès packstone à grainstone et wackestone se sont formées.

the Ece quarry (Claes *et al.*, 2015) and to the southern side in Best Abandoned and Alimoğlu quarries (Claes *et al.*, 2019). Similarly, the İllik quarry, located east of the Çakmak quarry, possesses slopes oriented to N and S. This quarry exhibits an E to W oriented small dome structure as outlined in Claes *et al.* (2019).

A fractured zone observed in the Best-Abandoned quarry may reflect a former spring system, being characterized by packstone to grainstone and wackestone of phytoclasts lithofacies which formed as vertical fracture in-fills indicating a circulation of fluids through fracture networks (Curewitz & Karson, 1997).

4.3.1.2 - Faber West travertine quarry

Description

The Faber West quarry consists of about 12.5 m thick boundstone of stromatolites, 17.5 m thick wackestone interfingered with packstone to grainstone and 5 m thick phytoherm of reeds from base to top, respectively (fig. 12). The boundstone of stromatolites form significantly extended pond environment, being developed in on a rough intraclastic packstone to grainstone surface. In this environment, less amount of wackestone of phytoclasts overlie the boundstone of stromatolites lithofacies (fig. 12). On the one side, lime muds, intraclasts and phytoclasts together occurs in marsh pool environment. The abundance of these phytoclasts and intraclastic layers together with the depth of microterraces increases from extended pond towards marsh pool (fig. 13). Palustrine deposits are characterized by an intense abundance of phytoherm of reeds and lime muds, overlying the marsh pools.

The Faber West quarry has a topographic slope of lower than 10º-20° varying from SW to NE (fig. 14A). This quarry is characterized by stratification of concave- to convex-shaped microterrace deposits that exhibit regular stacking, 25 to 35 m high and several hundreds of meters wide (fig. 14B-C) and is locally covered by Quaternary alluvial fan deposits being 20-meter-thick (fig. 14A).

Interpretation

Small obstacles of abundant phytoclasts, coated by lime muds, formed in calm marsh pools (Chafetz & Folk, 1984; Arenas *et al.*, 2010). High amount of phytoclasts present in these areas allows water flow direction to change, hereby leading to inclined intraclastic layers in places where water discharge either ceased or was insufficient (figs. 12 & 13). Coatings surrounding the phytoclasts which might be in the distal parts of an extended pond environment display clotted and pustular fabrics. These fabrics may point towards a high level of dissolved carbonate, which makes up irregular layers that were reported to form especially along the margins of lakes (Fort *et al.*, 1989; Dupraz *et al.*, 2009; Jahnert & Collins, 2013). On top of the marsh pool environment, a palustrine environment, characterized mainly by phytoherm of reeds lithofacies (Mohammadi *et al.*, 2020) exhibiting a spongy fabric of micritic stem-like forms, developed upward just over a thick surface with packstone to grainstone lithofacies (fig. 12).

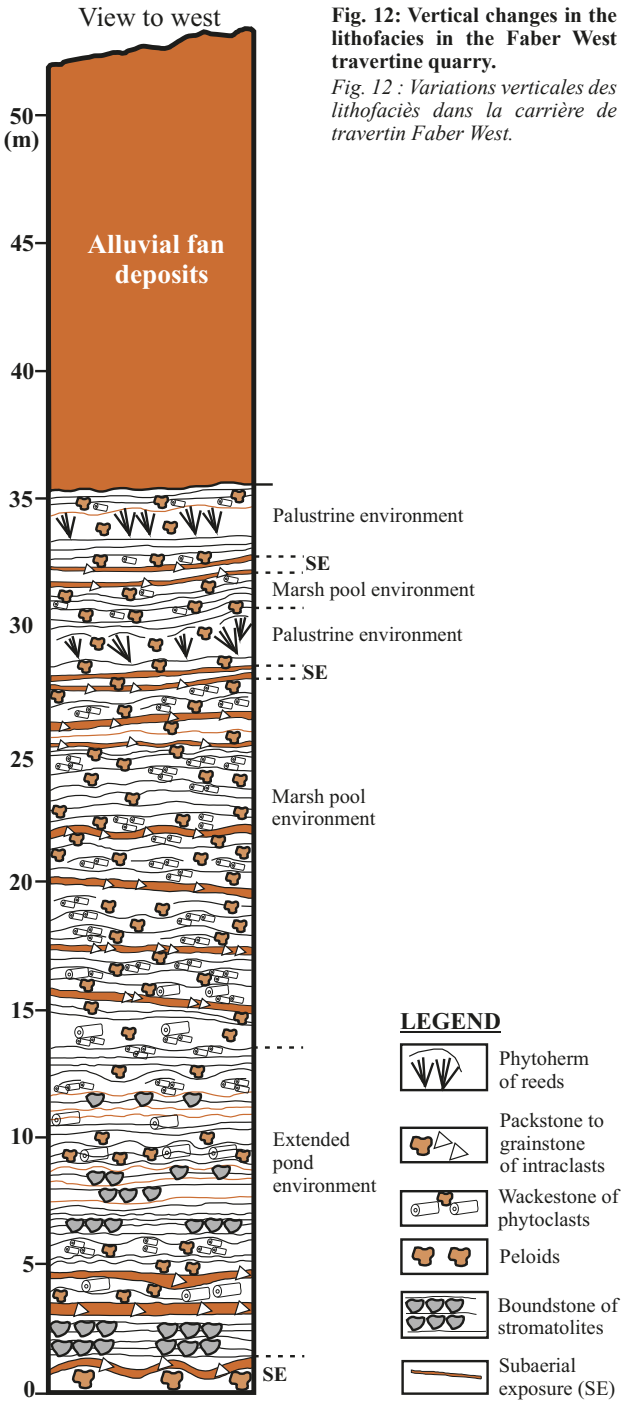

Fig. 12: Vertical changes in the lithofacies in the Faber West travertine quarry.
Fig. 12 : Variations verticales des lithofaciès dans la carrière de travertin Faber West.

Boundstone of stromatolites of distal slope and extended pond environments in Çakmak quarry (De Boever *et al.*, 2017; Mohammadi *et al.*, 2020) laterally continue in the Faber West quarry at the west side with no changes observed in the fabric of the lithofacies. Dilution of spring waters with freshwater took place away from the palaeospring locations, i.e. in the distal slope and lead to the growth of reeds, which resulted in packstone to grainstone lithofacies full with intraclasts (Guo & Riding, 1998). This is reflected by the layers of intraclastic packstone to grainstone lithofacies that were frequently encountered in the marsh pool areas (fig. 13).

4.3.1.3 - Demmer and Başaranlar travertine quarries

Description

Demmer quarry contains huge amount of packstone to

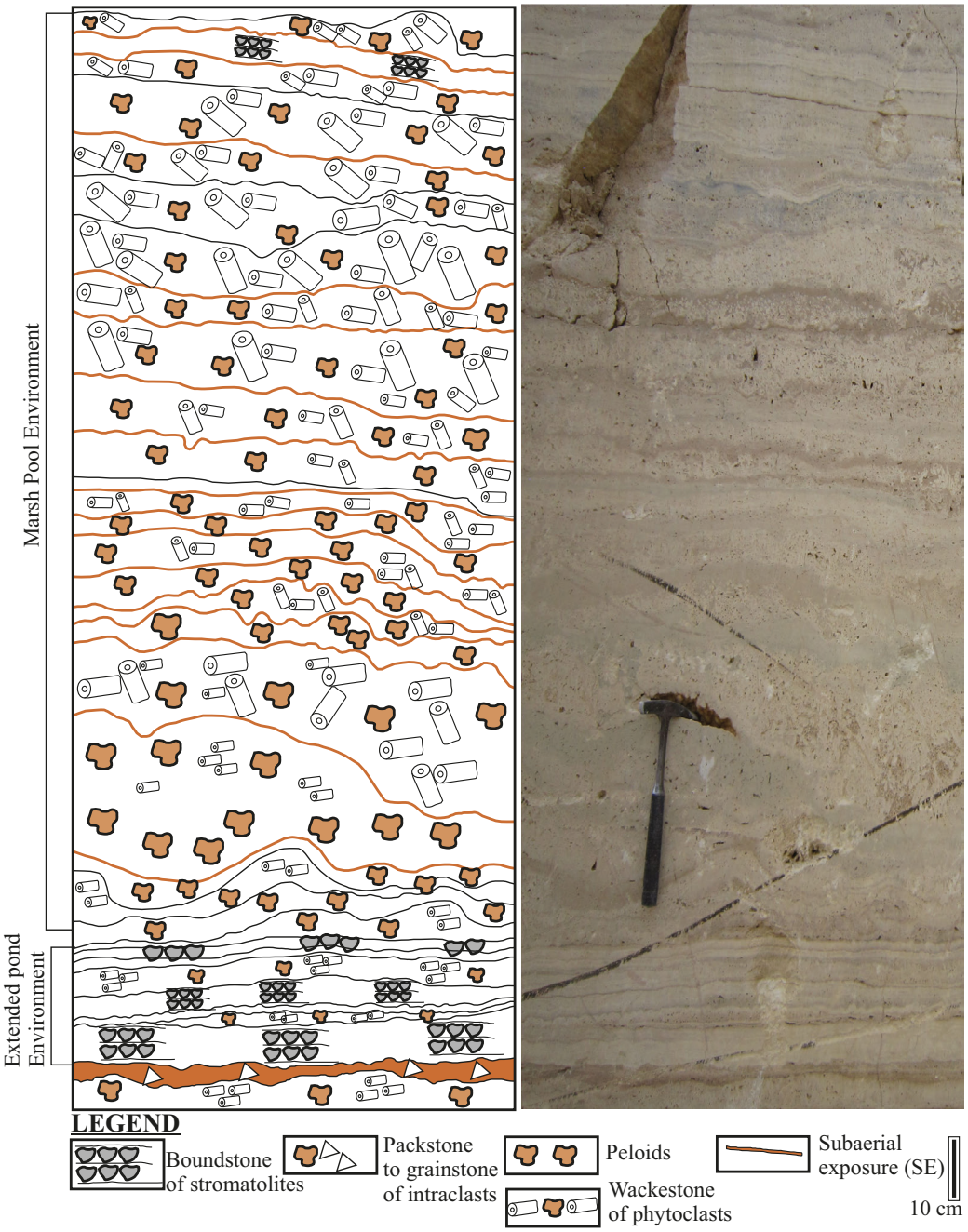

Fig. 13: Detailed lithofacies change from extended pond at the bottom to marsh pool environment above at the Faber West quarry.

Fig. 13 : Détail du changement de lithofaciès d'un environnement lacustre à la base à un environnement marécageux au-dessus dans la carrière Faber West.

grainstone of intraclasts and lime muds which interlayered with wackestone of phytoclasts and reed stems. Pseudo-fenestral pores are often observed between packstone to grainstone and wackestone lithofacies. They are typical for palustrine environment, whereas packstone to grainstone of gastropods increases from base to top, leading to a presence of marsh pool environment (fig. 15).

Başaranlar quarry is formed by packstone to grainstone with pseudo-fenestral pores, lime muds and intraclasts, phytoherm of bryophytes and wackestone of phytoclasts from base to top, respectively. Abundace of gastropods and intraclasts in packstone to grainstone lithofacies increases towards the east, and is an indicative of a flood plain environment (fig. 15).

These quarries, which formed in the most southeastern edge of the travertine geobody, are characterized by an alternation of disturbed to massive laminates up to 0.5 cm in thickness (fig. 14) and by a topographic gradient of at most 15º. Demmer quarry consists of marsh pool deposits which overlay palustrine sediments; whereas, Başaranlar quarry comprises of flood plain deposits which cover palustrine sediments (fig. 15).

Interpretation

Irregularly thick disturbed layers indicate high fluctuations in water flow, possessing abundant lime mud sedimentation, typical for marsh pool settings (e.g. Chafetz & Folk, 1984; Guo & Riding, 1998; Özkul *et al.*, 2002; Alonso-Zarza & Tanner, 2010; Toker *et al.*, 2016). Packstone to grainstone of gastropods lithofacies occur frequently in the latter environment that developed within marginal parts of a lacustrine setting under subaqueous conditions (Gierlowski-Kordesch, 2010). These marsh pools evolve eastward into a flood plain environment in which many gastropods, ostracods and charas were broken and are floating within micrite matrix indicating abundant lime mud sedimentation. Besides, most plants indicating palustrine environment occur together with reworked

Fig. 14: Depositional environments in the Faber West travertine quarry based on the lithofacies of the five excavation levels (L1 to L5).
A/ Depositional architecture. B/ Marsh pool environment with various lithofacies. C/ Alternating marsh pool and palustrine environments. Lithofacies: (1-5: packstone to grainstone of gastropods and intraclasts; 2-3: packstone to grainstone with more intraclasts; 6: boundstone of stromatolites; 8: phytoherm of reeds; 9: wackestone of phytoclasts.

Fig. 14 : Environnements de dépôt de la carrière de travertin Faber West basés sur les lithofaciès des cinq niveaux d'excavation (L1 à L5). A/ Structure des dépôts. B/ Environnement marécageux à lithofaciès variés. C/ Alternances entre environnements marécageux et palustres. Lithofaciès : 1-5 : packstone à grainstone avec gastéropodes et intraclastes ; 2-3 : packstone à grainstone avec plus d'intraclastes ; 6 : boundstone de stromatolites ; 8 : phytoherme de roseaux ; 9: wackestone de phytoclastes.

travertine particles. Quaternary fine-grained alluvial fan deposits and packstone to grainstone lithofacies of intraclasts could refer to the palustrine conditions with a limited water cover (fig. 15; Freytet & Verrecchia, 2002; Alonso-Zarza & Tanner, 2010).

4.3.2 - Depositional environment of travertine quarries at the Upper Domain

4.3.2.1 - Upper Tuna travertine quarry

Description

This quarry is characterized by an intercalation of brown- and grey-coloured lime muds, packstone to grainstone of gastropods and intraclasts as well as wackestone of phytoclasts. Grainstone of coated grains is found between packstone to grainstone lithofacies, coming over channel-fills deposits composed of sandstone, claystone, mudstone and conglomerate. In upper part of the quarry, wackestone lithofacies is overlain by fully lime muds of packstone to grainstone. The latter lithofacies is covered by a highly inclined thick marl deposit. Afterwards phytoherm of reeds lithofacies is developed, being overlain by packstone to grainstone of intraclasts, gastropods and wackestone of phytoclasts lithofacies (fig. 16). High amount of intraclasts, phytoclasts and broken gastropods refer to flooded plain and slope environments with irregular smooth layers having a thickness of 0.5 to 1 m. The marl deposit represents palustrine conditions in which many plants are developed. The phytoherm of reeds together with the packstone to grainstone of disseminated gastropods and intraclasts, which represent a total quantity of 50%, characterize the flooded slope environment with layers. These layers are inclined due to tectonic activity and the inclinaison varies between 10º and 20º (fig. 17A-B). The latter environment with an accumulation of slightly sloping irregular but smooth layers developed in a south to north direction (fig. 17B) whereas the flood plain environment pursued its extension from the west towards the east (fig. 17C).

Interpretation

Flooded slope and plain environments, as suggested by Lopez *et al.* (2017), likely result from short-lived

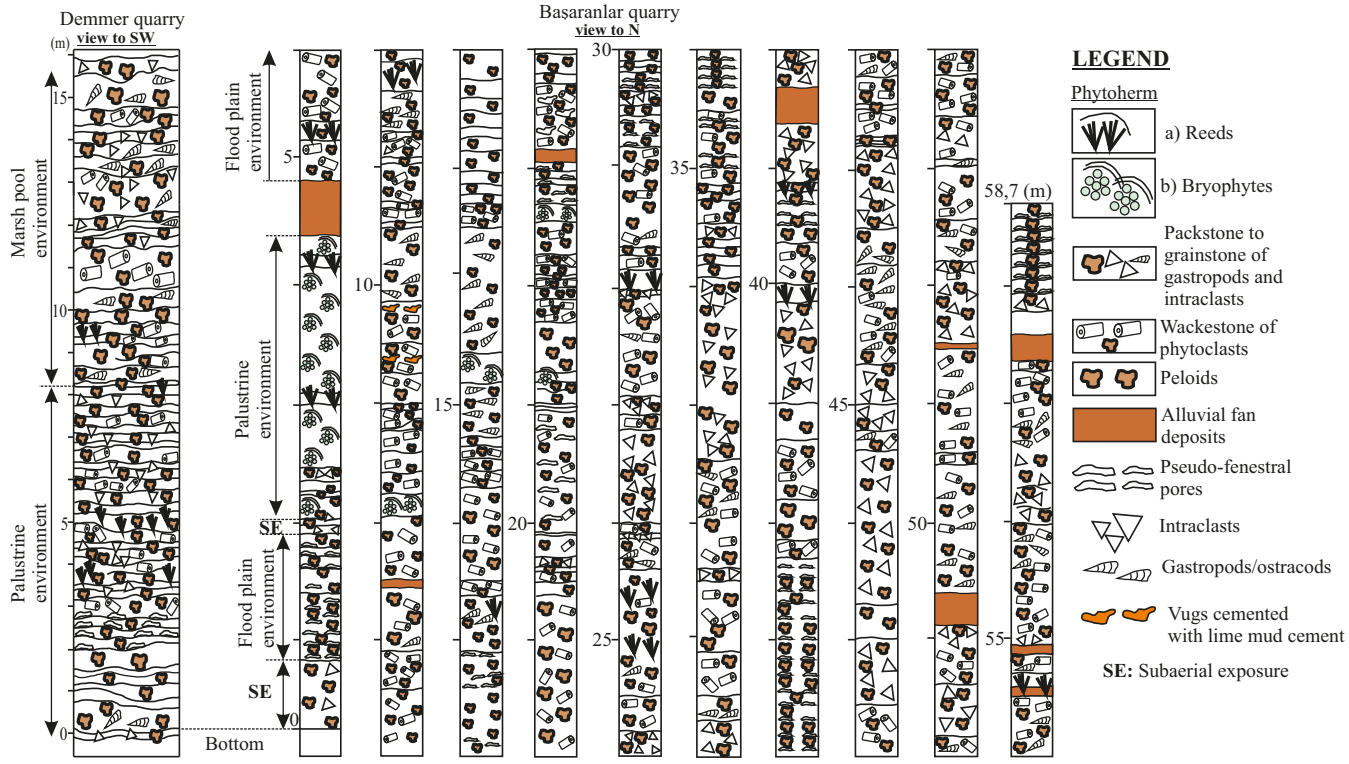

Fig. 15: Vertical lithofacies changes in the Demmer and Başaranlar travertine quarries (notice the different scales).
Fig. 15 : Evolution des lithofaciès dans les carrières de travertin de Demmer et Başaranlar (attention aux échelles différentes entre les deux sites).

pluvial events which led to an expansion of shallow lakes (Wright & Barnett, 2015). These events cause physical reworking of detrital components. From west to east, the flooded slope grades into flood plain deposits in which an intercalation of packstone to grainstone of brown- and grey-coloured lime muds with wackestone of phytoclasts mainly occurs (Bowen & Bloch, 2002; Vazquez-Urbez *et al.*, 2012). The short-lived pluvial events caused areas with pools and tectonic-induced slopes to become flooding. This flooding system was supported by baffling processes (Lopez *et al.*, 2017). On the one hand, the transition from flood system to palustrine environment can be attributed to baffling processes, as regularly recorded in tufa depositional systems (Martin-Algarra *et al.*, 2003; Pedley *et al.*, 2003; Pedley, 2009) since the flooded slope consists of packstone to grainstone lithofacies of intraclasts, gastropods floating within a lime mud matrix. High amount of disseminated gastropods, intraclasts and channel in-fills which developed within alluvial fans accumulated in the flood plain (Lopez *et al.*, 2017). The mixture of lenticular gastropods and intraclasts found as peloids, which form an irregular clotted fabric of packstone to grainstone lithofacies, and grainstone with coated grains lithofacies might suggest the former presence of a stream bed (Pedley *et al.*, 2000). These deposits are very similar to those in fluvial tufa systems as described by Ford and Pedley (1996) and Arenas *et al.* (2014). Similar fluvial channels that developed within the proximal alluvial fans system have been observed in the Eocene Peguera limestone of Mallorca Island in Spain (Arenas *et al.*, 2007).

4.3.2.2 - Kömürcüoğlu travertine quarry

Description

This quarry is highly made up by a systematic alternation of packstone to grainstone of gastropods, broken ostracods, charophytes and intraclasts with wackestone of phytoclasts lithofacies (fig. 18). In the upper part of the quarry, phytoherm of reeds and bryophytes lithofacies occurred, whereas at the bottom packstone to grainstone of coated grains have formed in the channel-fills deposits. In some cases, the packstone to grainstone of coated grains are intercalated with phytoherm of bryophytes which are surrounded by crust of dendrites in the southeast of the quarry (fig. 18). The channel in-fills ranging between 0.5 and 1.7 m in thickness correspond to laterally continous single channels. These in-fills consist of poorly sorted coarse sub-rounded conglomerates with different colours and sub-angular gravels.These particles were intercalated with brown-coloured less discontinous mud layers (fig. 18). The latter alluvial fan deposits occur within the west side of Kömürcüoğlu quarry and interfinger with wackestone of phytoclasts and packstone to grainstone of intraclasts, broken gastropods and coated grains with fibres reflecting a flooding system. Besides, grainstone of coated grains lithofacies is formed along channel-fills which have a thickness of 20 m in the west and can be massive or showing a complex-fill with stratified sedimentary structures (fig. 19).

Some lithofacies and fabric characteristics differ in flood plain and slope environments. Packstone to grainstone of coated grains (fig. 3I) covering phytoherms form in flooded slope to the west, while stratified packstone to grainstone of gastropods and intraclasts with pseudo-fenestral pores occur in flooded slope environment to the east (fig. 18).

The travertines exposed in this quarry display a lenticular to wedge-shaped, downslope-facing lobate geometry with a height/width ratio higher than 1 and asymmetrical flanks dipping lower than 45º (fig. 20). This quarry, developed NE-SW of Ballık, has a topographic slope

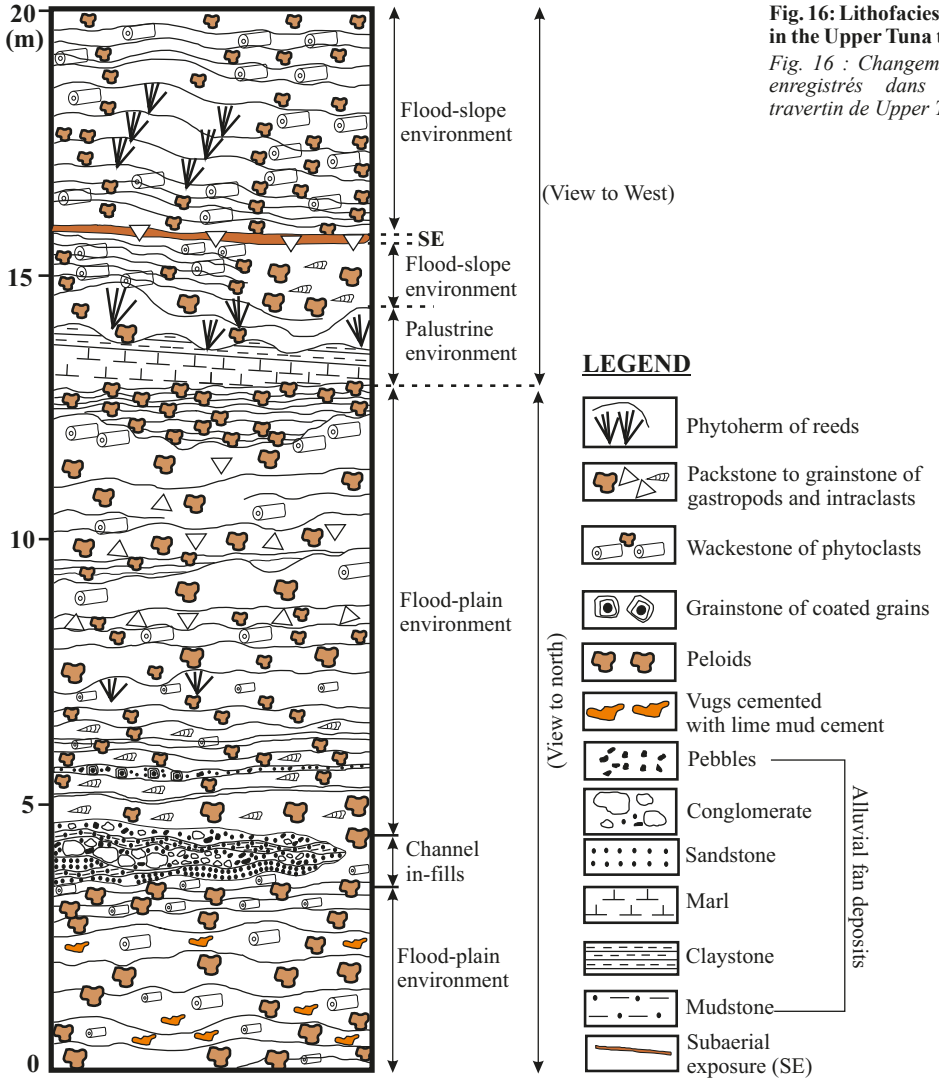

Fig. 16: Lithofacies changes recorded in the Upper Tuna travertine quarry.
Fig. 16 : Changements de lithofaciès enregistrés dans la carrière de travertin de Upper Tuna.

ranging between 20º and 40º and a width of about 750 m. It exhibits various sub-environments characteristics from bottom to quarry top, namely: flood plain, flooded slope and palustrine, respectively (figs. 18 & 20). The flood plain environment, which is up to 30 m thick, represents a middle part of lobe close to possible spring vent. It is characterized by an irregular stacking of smooth to micro-terraced layers. The flood plain is starting from the north side of the quarry and evolves into flooded slope with a thickness of 20 m towards the southeast (fig. 21). Large cavities and fractures have especially been observed in the northwest of the Kömürcüoğlu quarry (fig. 21).

Interpretation

Kömürcüoğlu quarry has a mound-shaped morphology as the spring water was discharged from the highest point. The cross-section of mound exhibits a lobe geometry (Van Noten *et al.*, 2019). In this mound, there is a laterally sharp transition from flood plain environment towards flooded slope environment. The lateral variation reflects downlapping progradation which was developed as the base level of precursor stream bed drops (Martin-Algarra *et al.*, 2003; Pedley *et al.*, 2003). In addition, successive progradation of lobes could lead to different depositional geometries (fig. 20). This can be due to high sedimentation rate and water quantity conditions when vegetation density is high (Arenas *et al.*, 2014) and may reflect channelled pool terrace bodies, well-established in palustrine flood plain settings with pools and drainage channels as reported in literature (Pedley, 1990; Violante *et al.*, 1994; Vazquez-Urbez *et al.*, 2012). Packstone to grainstone of coated grains that occur in the form of microterraces in flooding slopes can be associated with periodic variations in water flow which influences calcite sedimentation (*sensu* Guo & Riding, 1998; Pentecost, 2005; Erthal *et al.*, 2017). The fact that these layers frequently interlayer with intraclast-rich packstone to grainstone in flood plain and slope settings, may reflect periodic fluctuations in water discharge. Laminar water flow along flooded slopes and away from high gradient of topography could form columnar- and flat-laminated fabrics representing stromatolite-like layers formed within the packstone to grainstone of coated grains (Rainey & Jones, 2009; Croci *et al.*, 2016; Erthal *et al.*, 2017). In contrast, agitated waters developed where channel bodies with alluvial fan deposits transit into flooded slope environments (fig. 21) and gave rise to coated grains composed of coatings with dendrites and peloidal nuclei in the packstone to grainstone to be formed as a result of turbulence-induced CO_2 degassing (*sensu* Folk *et al.*, 1985; Rainey & Jones, 2009; Brasier, 2011; Okumura *et al.*, 2012). An alternation of packstone to grainstone of gastropods and intraclasts and wackstone of phytoclasts lithofacies increases towards the east of

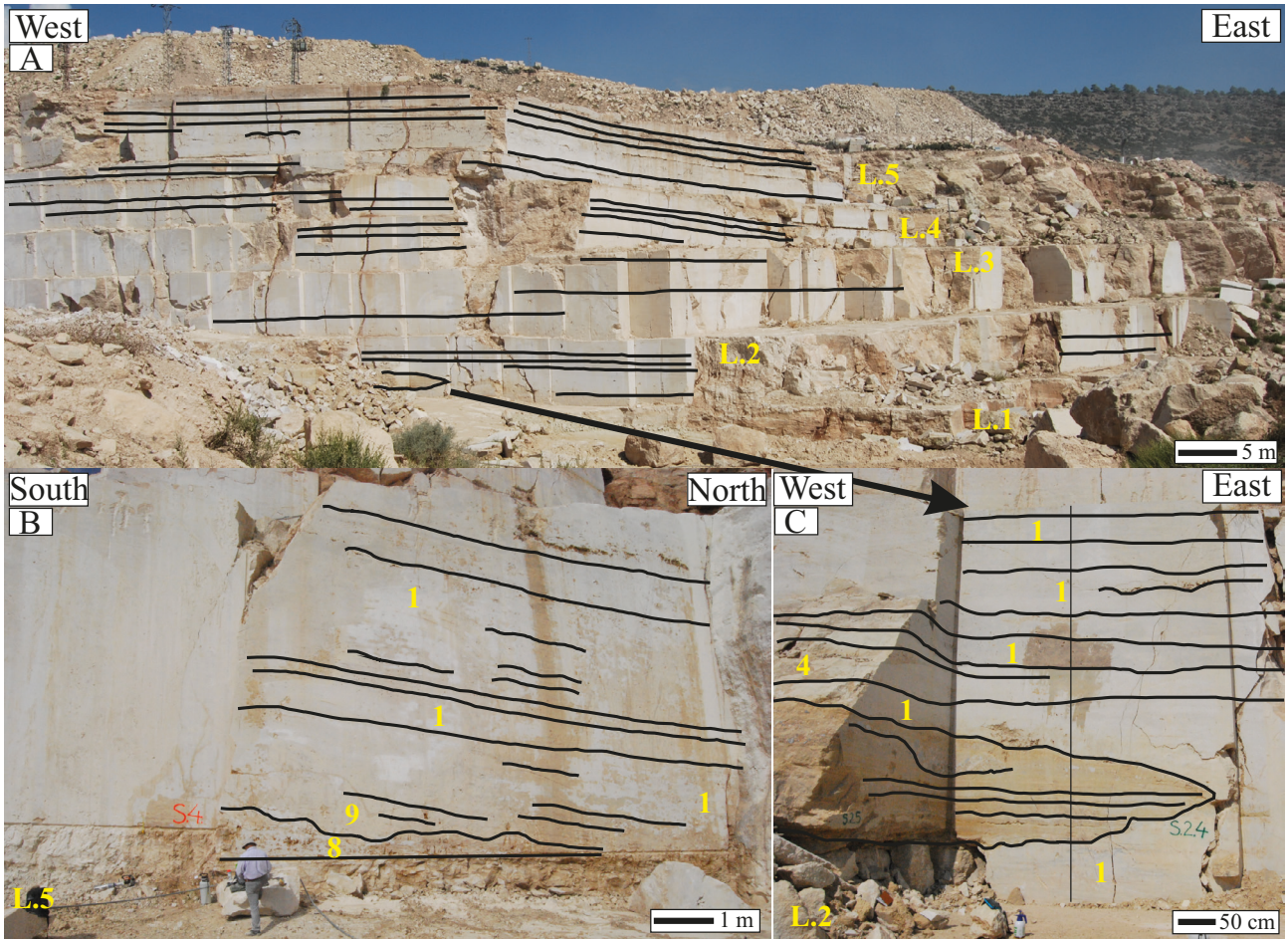

Fig. 17: Depositional architecture in the Upper Tuna travertine quarry throughout the five excavation levels (L1 to L5).
A/ Depositional architecture. B/ Detail of flooded slope environments (1: packstone to grainstone with gastropods and intraclasts; 9: Wackestone of phytoclasts) formed over palustrine environment (8: phytoherm of reeds developed over marls). C/ Detail of channels infillings formed within flood plain environment (1: packstone to grainstone of gastropods and intraclasts; 4: grainstone of coated grains lithofacies).
Fig. 17 : Structure des dépôts dans la carrière de travertin Upper Tuna à travers les cinq niveaux d'excavation (L1 à L5). A/ Structure des dépôts. B/ Détail des dépôts de pente inondée (1 : packstone à grainstone à gastéropodes et intraclastes ; 9 : wackestone de phytoclates) formés sur un environnement palustre (8 : phytoherme de roseaux développé sur des marnes). C/ Détail des remplissages de canaux formés dans un environnement de plaine inondable (1 : packstone à grainstone de gastéropodes et intraclastes; 4 : grainstone de grains enrobés).

this quarry. They likely indicate the periodically influence of flood discharge from the east side (fig. 19; Vazquez-Urbez *et al.*, 2012). In contrast, when no flooding is seasonally developed shallow waters would have led to lime mud sedimentation and bioturbation by roots (fig. 3C; Vazquez-Urbez *et al.*, 2012; Erthal *et al.*, 2017). Furthermore, the signs of the bioturbation and pores between peloids which form an irregular clotted fabric of packstone to grainstone of gastropods could reflect a major contribution of microorganisms and vegetation in the flood plain environment.

A set of constructing macrophytes, such as reeds, grasses, bryophytes or mosses were encrusted in growth position (Weijermars *et al.*, 1986; Pedley, 1990; Violante *et al.*, 1994) nearby these alluvial fan deposits. The phytoherms indicate typically the presence of a palustrine environment and might be formed in peripheral margin of lobes (Pedley *et al.*, 2003; Arenas *et al.*, 2007). Shallow pools, which developed immediately behind the resulting small obstacles, were filled by phytoclasts and liverworts bearing wackestone lithofacies and gastropods along with abundant packstone to grainstone of intraclasts lithofacies. Large cavities and fractures (fig. 3H) may reflect non-selective dissolution of bioconstructed plants within the vadose zone where this dissolution could have happened when the water table was lowered in flood plain and slope environments (Pedley *et al.*, 2003). At this time, the resulting pores were filled by considerable abundance of intraclasts, extraclasts, intercalated with lime muds in packstone to grainstone lithofacies due to the dismantling of travertines (fig. 21). Higher erosion results when flow direction of spring waters changes, leading to presence of more intraclasts (fig. 3D) and wackestone of phytoclasts lithofacies (fig. 3F), which appears as an accumulation of encrusted plant debris (Pedley, 2009).

Considering the fact that Kömürcüoğlu travertine quarry is typically characterized by lateral heterogeneous depositional environments displaying a lobe geometry, the productivity of less fractured, massive travertine masses have been expected to be more facilitated in deeper and distal parts of this quarry where flood plain and slope environments existed.

5 - DISCUSSION

5.1 - Evaluation of Ballık travertine architecture

The Ballık area was subdivided into a "Lower and Upper domain" that have respectively a maximal elevation of 500 m and 877 m above sea level (Guo &

Riding, 1998; Van Noten *et al.*, 2019). Two large-scale faults, namely Killik and Düzçalı, separate these domains (fig. 22A). The Killik fault surrounded the south border of Killik hill in the "Lower Domain" (fig. 22A; Swennen *et al.*, 2017; Van Noten *et al.*, 2019). The Düzçalı strike-slip reactivation was associated with a number of normal faults developed perpendicular to the Düzçalı fault in the "Upper Domain" (Van Noten *et al.*, 2019). Taşkestik hill represents the highest topographic elevation in the latter domain. Van Noten *et al.* (2019) stated the hill may have

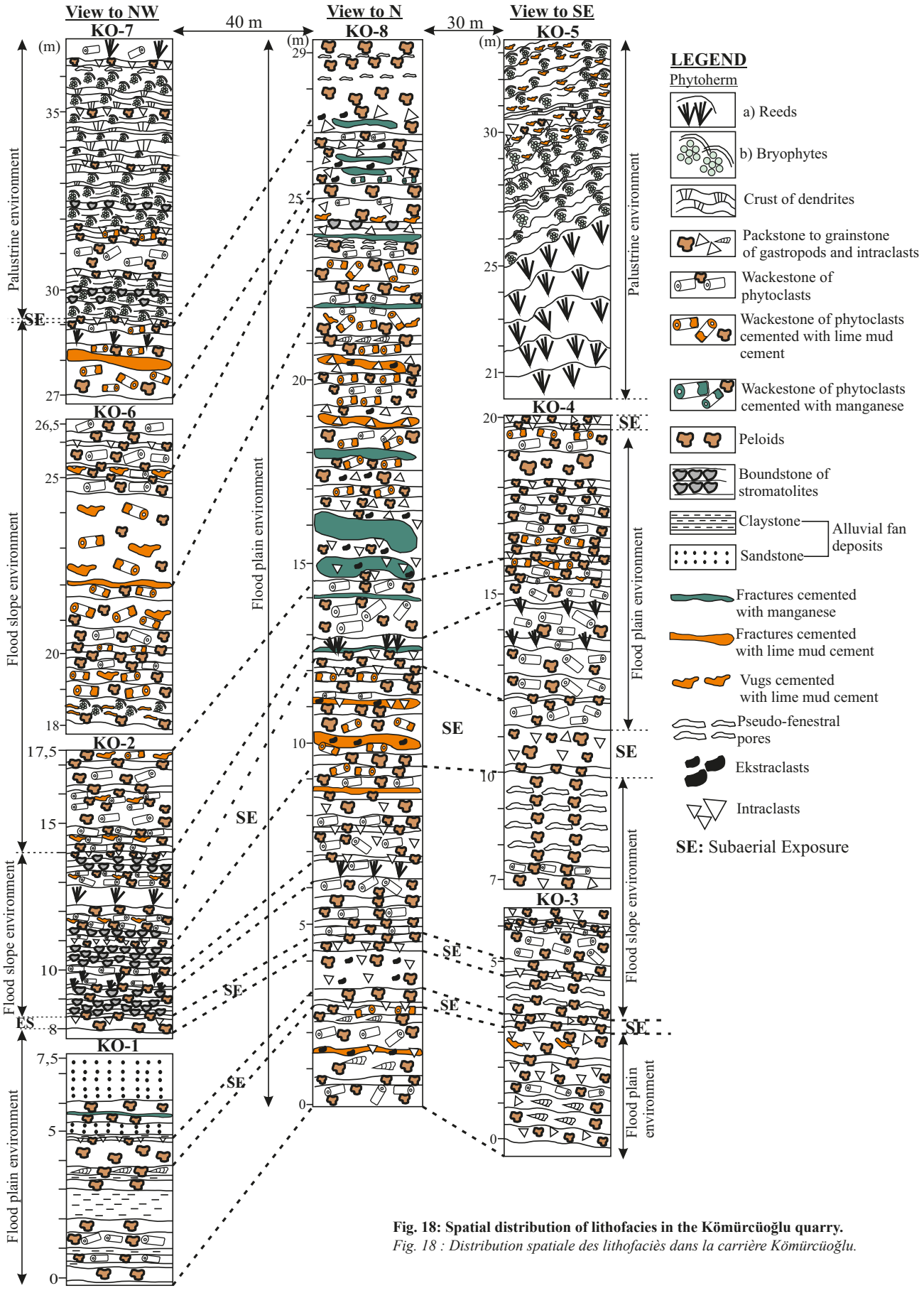

Fig. 18: Spatial distribution of lithofacies in the Kömürcüoğlu quarry.
Fig. 18 : Distribution spatiale des lithofaciès dans la carrière Kömürcüoğlu.

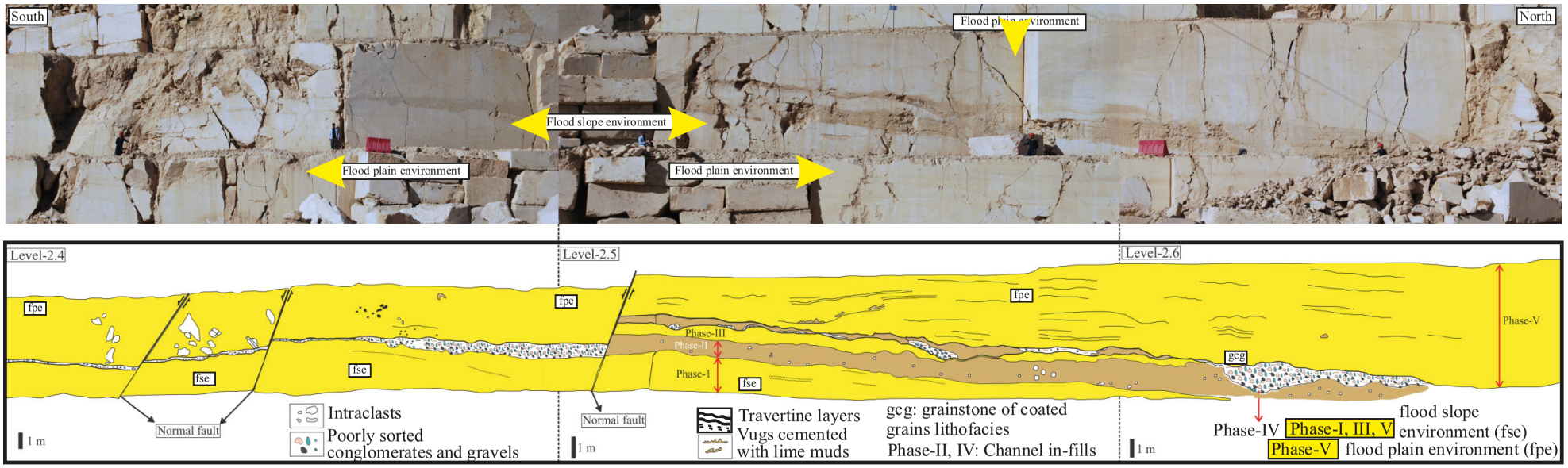

Fig. 19: Channel infillings formed within a flooded slope depositional environment in the west side of the Kömürcüoğlu travertine quarry.
Fig. 19 : Chenaux de remplissage formés dans un environnement de dépôt de pente inondée dans la partie ouest de la carrière de travertin Kömürcüoğlu.

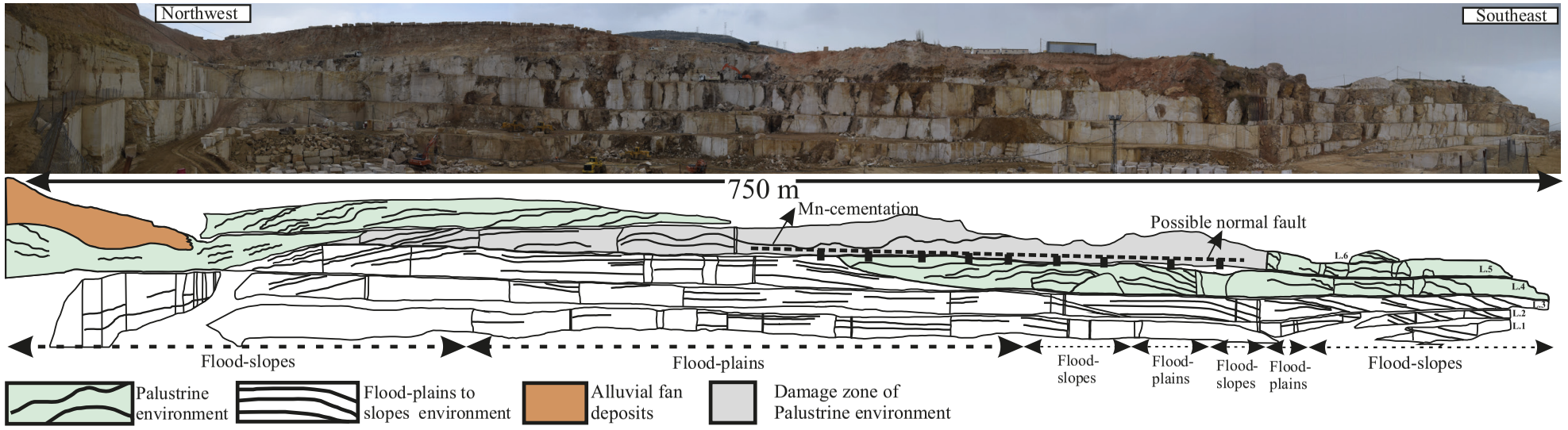

Fig. 20: Depositional architecture of the Kömürcüoğlu travertine quarry.
Fig. 20 : Structure des dépôts sédimentaires de la carrière de travertin Kömürcüoğlu.

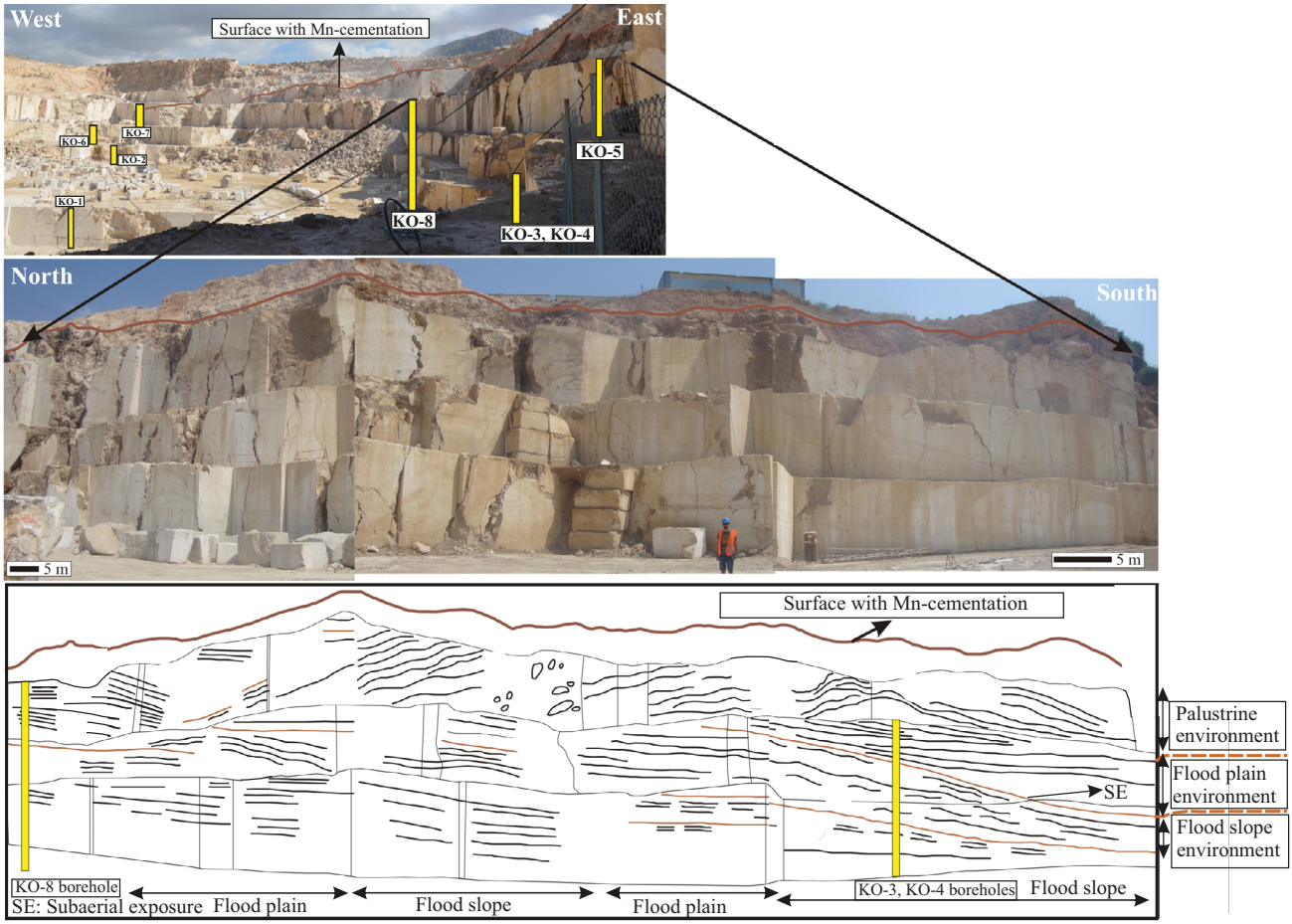

Fig. 21: Cross-section that illustrating the lateral variability of depositional environments in the Kömürcüoğlu travertine quarry.
Yellow columns indicates borehole locations.
Fig. 21 : Coupe transversale illustrant la variabilité latérale des environnements de dépôt dans la carrière de travertin Kömürcüoğlu. Les colonnes jaunes indiquent l'emplacement des forages.

resulted from uplift during the late Pleistocene-Holocene resulting in Quaternary alluvial fan deposits. It formed along the south-facing flank next to the Düzçalı fault (fig. 22B; Van Noten *et al.*, 2019).

5.1.1 - Spatial distribution of depositional environments in the "Lower Domain"

Lower Domain encompasses an extensive distribution of proximal to distal slope with a topographic gradient of 20-40° (Claes *et al.*, 2015; De Boever *et al.*, 2017), extended pond and marsh pool environments with a slope of 10-20° (fig. 22A) due to tectonic activity after travertine precipitation. However, these environments were changed to flood plain and palustrine environments, varying between 0° and 20° in a topographic slope, towards the east part (fig. 22B). Significantly precipitated boundstone lithofacies in extended pond environment implies that spring water precipitating travertine at the İllik and Alimoğlu quarries can harbour mainly thermal-sourced CO_2. This lithofacies can be connected to the bottom part of Faber West quarry. From these quarries towards Best Abandoned and Demmer-Başaranlar quarries, the spring water may become groundwater with meteoric-sourced CO_2 owing to the absence of boundstone and high abundance of packstone to grainstone lithofacies with intraclasts and wackestone of phytoclasts. These lithofacies characterize mainly marsh pool and flood plain environments. Della Porta (2015) suggested plant growths predominate in areas where groundwater and thermally generated spring water are discharged together. These waters can emerge in various locations of Lower Domain with an activation of few small-magnitude earthquakes in Ballık area (Guo & Riding, 1998; Della Porta, 2015; Van Noten *et al.*, 2019). So, on the top of Best Abandoned quarry between Alimoğlu and Demmer-Başaranlar travertine quarries a new spring system, filled by packstone to grainstone of intraclasts characterizing the marsh pool, might have been found (fig. 22B). In areas close to this spring system where topographic gradient is low, proximal slope environment with small individual pools in which reeds grew was formed. High discharge of the upwelling ground and spring waters in low relief areas of Lower Domain led to hill wash processes (Guo & Riding, 1998; Alonso-Zarza & Wright, 2010). The calcium bicarbonate-rich water precipitating travertine is reduced in Başaranlar quarry towards the most southeastern margin of the domain. This is supported by the absence of normal faults and high input of alluvial fan deposits (Alonso-Zarza & Wright, 2010; Van Noten *et al.*, 2019). In contrast, the Demmer quarry, close to Alimoğlu travertine quarry, achieved a high flow rate to be able to precipitate packstone to grainstone of gastropods lithofacies in marsh pool environment. The latter environment might have been connected laterally to marsh pool environment of Alimoğlu travertine quarry. This environment may evolve laterally into

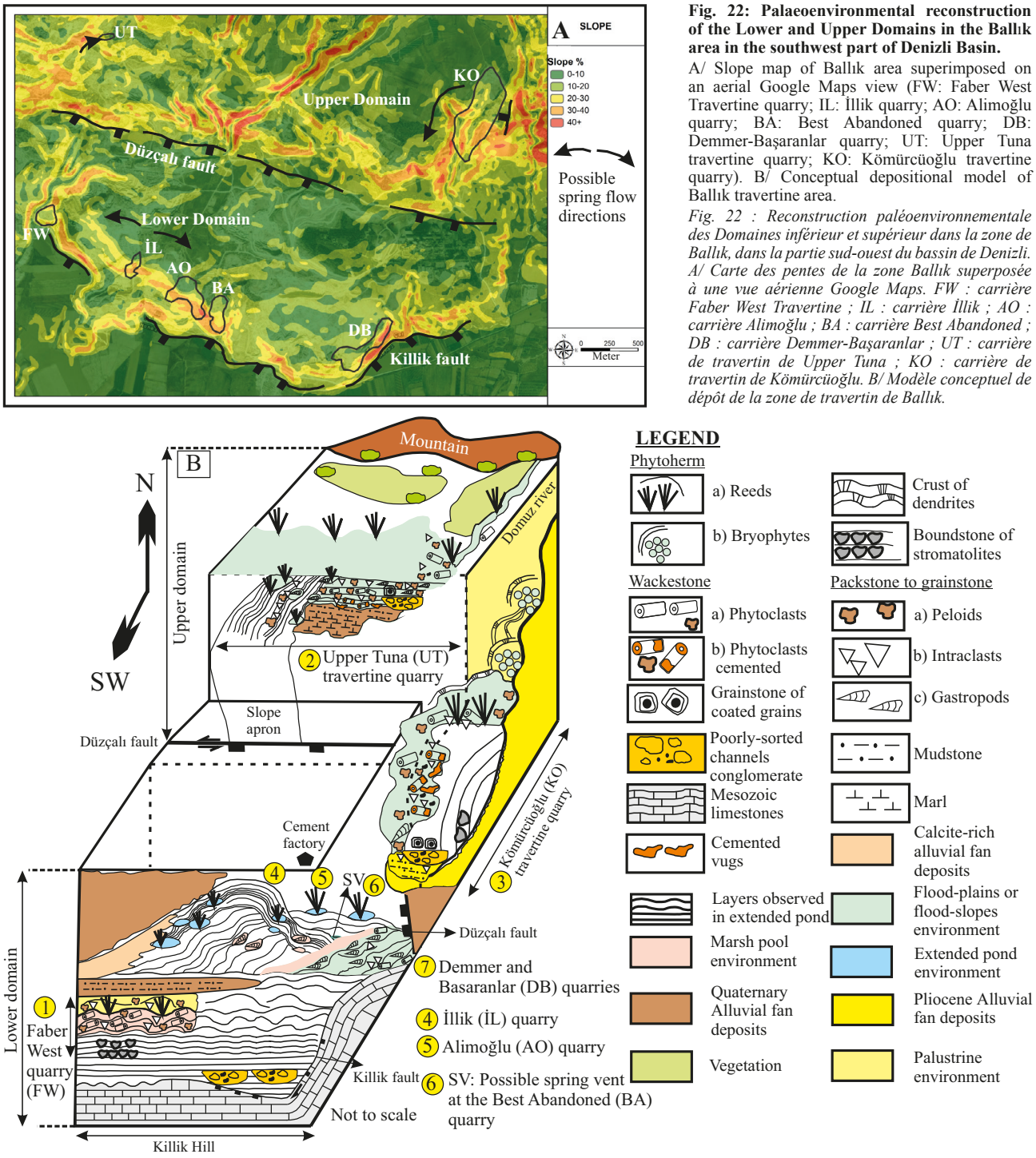

Fig. 22: Palaeoenvironmental reconstruction of the Lower and Upper Domains in the Ballık area in the southwest part of Denizli Basin.

A/ Slope map of Ballık area superimposed on an aerial Google Maps view (FW: Faber West Travertine quarry; IL: İllik quarry; AO: Alimoğlu quarry; BA: Best Abandoned quarry; DB: Demmer-Başaranlar quarry; UT: Upper Tuna travertine quarry; KO: Kömürcüoğlu travertine quarry). B/ Conceptual depositional model of Ballık travertine area.

Fig. 22 : Reconstruction paléoenvironnementale des Domaines inférieur et supérieur dans la zone de Ballık, dans la partie sud-ouest du bassin de Denizli. A/ Carte des pentes de la zone Ballık superposée à une vue aérienne Google Maps. FW : carrière Faber West Travertine ; IL : carrière İllik ; AO : carrière Alimoğlu ; BA : carrière Best Abandoned ; DB : carrière Demmer-Başaranlar ; UT : carrière de travertin de Upper Tuna ; KO : carrière de travertin de Kömürcüoğlu. B/ Modèle conceptuel de dépôt de la zone de travertin de Ballık.

flood plain environment in the Başaranlar quarry due to flooding event (fig. 22B). This event led to fluctuations in discharge of spring water and groundwater, reworking plants and travertine materials from Alimoğlu travertine quarry. Furthermore, it may form a small hill in the eastern part (fig. 22A-B).

The flood plains and palustrine environments in the east are more influenced by the input of fine-grained alluvial fan deposits than those of the west side, although the west side of these quarries has the thickest alluvial fan deposits (fig. 22B). Claes *et al.* (2015) and Mohammadi *et al.* (2020) stated that a mixing of ground and spring waters through the Lower Domain was induced by irregular variations of isotope signatures acquired both from micrite and cements.

5.1.2 - Spatial distribution of depositional environments in the "Upper Domain"

No marsh pool and extended pond environments recognised in the "Lower Domain" have been observed in the "Upper Domain" (fig. 22B). Travertine deposits in the latter domain have similar characteristics. However, they can be formed in areas of different topographic gradient and by spring waters that rose up from both Düzçalı fault and a normal fault perpendicular to Kömürcüoğlu fault (fig. 22A). A north-facing slope apron is characterized by flooded slope and palustrine environments with a topographic slope of 0-20° which evolve eastwards to flood plain environment in Upper Tuna quarry (fig. 22B). On the higher topographic gradient of 20-40°, the Upper Tuna travertine deposits changes to the Kömürcüoğlu

travertine deposits which most likely developed over an abandoned and faulted stream bed (fig. 22A-B). Due to the fact that the flood plain and slope along with palustrine are prominent environments in the most east part of "Upper Domain", the west and east areas must be seasonally flooded during different times. Flooding event must have led to different erosions in such high-gradient areas (Chafetz & Folk, 1984; Arenas *et al.*, 2007) since Pliocene alluvial fan deposits just surrounded the Kömürcüoğlu travertine quarry in the east unlike Upper Tuna quarry in the west (fig. 22B). The higher erosion allowed significantly packstone to grainstone lithofacies and wackestone of abundant phytoclasts and vugs infilled by sediments to be developed in the Kömürcüoğlu quarry.

6 - CONCLUSIONS

In this study six lithofacies were determined considering to six sedimentary characteristics that allowed to reconstruct a paleoenvironmental model of Ballık travertine quarries in the "Lower and Upper Domains" of the Denizli Basin. A slope map, applied to Ballık area, supports the distinction of a "Lower Domain" with İllik, Alimoğlu, Best Abandoned, Faber West, Demmer and Başaranlar travertine quarries from an "Upper Domain" with Upper Tuna and Kömürcüoğlu travertine quarries.

The "Lower Domain" exhibits a more heterogeneous environmental distribution, developed towards the west and east edges, although its subaqueous part reflects small-scale changes in terms of depositional environment. Complex lateral arrangements of marsh pool, extended pond and flood plain environments in this domain developed from Faber West quarry towards Demmer-Başaranlar quarry. Large-scale changes in the environment may account for a variable saturation of carbonate sedimentation and mutual discharges of spring and ground waters issuing on the slopes with low relief of Alimoğlu travertine quarry, which developed along the main Killik large-scale fault. Towards the eastern part of Lower Domain, decreasing travertine precipitation temperature and CO_2 degassing due to mixture of spring and ground waters can be attributed to (i) the increasing wackestone of phytoclasts (ii) high abundance of packstone to grainstone of intraclasts and gastropods, (iii) changing of smooth or micro-terraces to crinkly or disturbed layers, and (iv) variations of the coating fabrics of coated grains having radial fibres to irregular clotted fabrics of peloids in the packstone to grainstone lithofacies.

The "Upper Domain" has laterally homogeneous environments that consist of flood plain and flooded slope within Upper Tuna and Kömürcüoğlu travertine quarries. The dominance of the flood plain and slope environments in this domain can be related to low discharge of spring waters rising from two different faults, namely Düzçalı and a normal fault that developed near to Kömürcüoğlu fault, and to high input of alluvial fan deposits. Such a discharge from topography with high slope might create a laminar flow with slope breaks, thus leading to lateral and vertical systematic alternation of flood plain and slope environments in the Kömürcüoğlu travertine quarry. Besides alternating coated grains and intraclasts, accompanied by gastropods, in packstone to grainstone lithofacies were formed closer to spring system at the northwest side of the Kömürcüoğlu quarry. Phytoherm of reeds and bryophytes, which are surrounded by crust of dendrites, along with abundant lime muds, points to a palustrine environment in which very shallow waters seeping from possible springs accumulated.

ACKNOWLEDGEMENTS

The authors are grateful to Petrobras (Brazil) for financial support and permission to publish the data based on which this paper relies. Some fieldwork was supported by a travertine reservoir analogue project supported by Shell, Total and Petrobras. Boreholes from Kömürcüoğlu quarry were drilled in the framework of the 2017FEBE009 project. I am very grateful to the reviewer, Dr. Alvaro Rodriguez Berriguete, for helping me to improve the manuscript. The first author will be honored to give this paper as a gift to my mum, Şengül Aratman, since she passed away the moment I was working on this manuscript. During field work and sampling, I acknowledge the help and high performance of Mr. Levent Erkuş, an internship student in Pamukkale University, and Mrs. Marleen Bouman, master student from KU Leuven. It was a real pleasure to discuss the resulting palaeoenvironmental model with my colleagues, Dr. Dominique Jacques, Mr. Michael Verbiest and Mr. Alexander Minor, from the Geology Division of KU Leuven and Mr. M. Onur Ayaz from Mitto Consultancy of Turkey. Mr. Herman Nijs is acknowledged for the preparation of many high quality thin-sections. I am thankful to Mr. Turgay Çelik and Mr. Tuğrul Beyaz since they provided adequate facilities in Sedimentology and Reservoir Department of TPAO Research Center during the SEM analyses of the samples.

REFERENCES

ALÇİÇEK H., VAROL B. & ÖZKUL M., 2007 - Sedimentary facies, depositional environments and paleogeography evolution of the Neogene Denizli Basin, SW Anatolia, Turkey. *Sedimentary Geology*, **202**, 596-637.

ANADON P., UTRILLA R. & VAZQUEZ A., 2000 - Use of charophyte carbonates as proxy indicators of subtle hydrological and chemical changes in marl lakes: example from the Miocene Bicorb Basin, eastern Spain. *Sedimentary Geology*, **133**, 325-347.

ALTUNEL E. & HANCOCK P.L., 1993 - Morphological features and tectonic setting Quaternary travertines at Pamukkale, Western Turkey. *Geological Journal*, **28**, 335-346.

ALONSO-ZARZA A.M. & TANNER L.H., 2010 - *Carbonates in continental settings: Facies, environment and processes*. Developments in Sedimentology, **61**, Elsevier, Amsterdam, 400 p.

ALONSO-ZARZA A.M. & WRIGHT V.P., 2010 - Palustrine carbonates. *In* A.M. Alonso-Zarza & L.H. Tanner (eds.), *Carbonates in continental settings: Facies, environments and processes*. Developments in Sedimentology, **61**. Elsevier, Amsterdam, 116-118.

ARENAS C., CABRERA L. & RAMOS E., 2007 - Sedimentology of tufa facies and continental microbialites from the Palaeogene of Mallorca Island (Spain). *Sedimentary Geology*, **197**, 1-27.

ARENAS C., GUTIERREZ F., OSACAR C. & SANCHO C., 2000 - Sedimentology and geochemistry of fluvio-lacustrine tufa deposits controlled by evaporite solution subsidence in the central Ebro Depression, NE Spain. *Sedimentology*, **47**, 883-909.

ARENAS C., VAZQUEZ-URBEZ M., PARDO-TIRAPU G. & SANCHO-MARCEN C., 2010 - Fluvial and associated carbonate deposits, *In* A.M. Alonso-Zarza & L.H. Tanner (eds.), *Carbonates in continental settings: Facies, environments and processes*. Developments in Sedimentology, **61**. Elsevier, Amsterdam, 138-145.

ARENAS C., VAZQUEZ-URBEZ M., PARDO G. & SANCHO C., 2014 - Sedimentology and depositional architecture of tufas deposited in stepped fluvial systems of changing slope: Lessons from the Quaternary Anamaza Valley (Iberian Range, Spain). *Sedimentology*, **61**, 133-171.

BAHNIUK A.M., ANJOS S., FRANCA A.M., MATSUDA N., EILER J., MCKENZIE J.A. & VASCONCELOS C., 2015 - Development of microbial carbonates in the Lower Cretaceous Codo Formation (north-east Brazil): Implications for interpretation of microbialite facies associations and palaeoenvironmental conditions. *Sedimentology*, **62**, 155-181.

BRASIER A.T., 2011 - Searching for travertines, calcretes and speleothems in deep time: Processes, appearances, predictions and the impact of plants. *Earth-Science Reviews*, **104**, 213–239.

BOWEN G.J. & BLOCH J.I., 2002 - Petrography and geochemistry of floodplain limestones from the Clarks Fork basin, Wyoming, USA: carbonate deposition and fossil accumulation on a Paleocene-Eocene floodplain. *Journal of Sedimentary Research*, **72**, 46-58.

CAPEZZUOLI E., GANDIN A. & PEDLEY M., 2014 - Decoding tufa and travertine (fresh water carbonates) in the sedimentary record: The state of the art. *Sedimentology*, **61**, 1-21.

CERALDI T.S. & GREEN D., 2016 - Evolution of South Atlantic lacustrine deposits in response to Early Cretaceous rifting, subsidence and lake hydrology. *In* S. Ceraldi, R.A. Hodgkinson & G. Backe (eds.), *Petroleum Geoscience of the West Africa Margin*. Geological Society, London, Special Publications, 438 p.

CHAFETZ H.S. & FOLK R.L., 1984 - Travertines: Depositional Morphology and The Bacterially Constructed Constituents. *Journal of Sedimentary Geology*, **54**, 289-316.

CHAFETZ H.S. & GUIDRY S. A., 1999 - Bacterial shrubs, crystal shrubs, and ray-crystal shrubs: Bacterial vs. abiotic precipitation. *Sedimentary Geology*, **126**, 57-74.

CHEN J., ZHANG D.D., WANG S., XIAO T. & HUANG R., 2004 - Factors controlling tufa deposition in natural waters at waterfall sites. *Sedimentary Geology*, **166**, 353-366.

CLAES H., SOETE J., VAN NOTEN K., EL DESOUKY H., MARQUES ERTHAL M., VANHAECKE F. ÖZKUL M. & SWENNEN R., 2015 - Sedimentology, three-dimensional geobody reconstruction and carbon dioxide origin of Pleistocene travertine deposits in the Ballık area (south-west Turkey). *Sedimentology*, **62**, 1408-1445.

CLAES, H., HUYMANS, M., SOETE, J., DIRIX, K., VASSILIEVA, E., ERTHAL, M.M., VANDEWIJNGAERDE, W., HAMAEKERS, H., ARATMAN, C., ÖZKUL, M. & SWENNEN, R., 2019 - Elemental geochemistry to complement stable isotope data of fossil travertine: Importance of digestion methods and statistics. Sedimentary Geology, 386, 118-131.

CROCI A., DELLA PORTA G., CAPEZZUOLI E., 2016 - Depositional architecture of a mixed travertine-terrigenous system in a fault-controlled continental extensional basin (Messinian, Southern Tuscany, Central Italy). *Sedimentary Geology*, 332, 13-39.

CUREWITZ D. & KARSON J.A., 1997 - Structural settings of hydrothermal outflow: fracture permeability maintained by fault propagation and interaction. *Journal of Volcanology and Geothermal Research*, **79**, 149-168.

DE BOEVER E., FOUBERT A., LOPEZ B., SWENNEN R., JAWOROWSKI C., ÖZKUL M. & VIRGONE A., 2017 - Comparative study of the Pleistocene Cakmak quarry (Denizli Basin, Turkey) and modern Mammoth Hot Springs deposits (Yellowstone National Park, USA). *Quaternary International*, **437**, 129-146.

DELLA PORTA G.D., 2015 - Carbonate build-ups in lacustrine, hydrothermal and fluvial settings: comparing depositional geometry, fabric types and geochemical signature. *In* D.W.J. Bosence, K.A. Gibbons, D.P. Le Heron, W.A. Morgan, T. Pritchard, B.A. Vining (eds.), *Microbial Carbonates in Space and Time: Implications for Global Exploration and Production*. Special Publications - Geological Society, **418**. Geological Society of London, London, 17-68.

DUNHAM R.J., 1962 - Classification of carbonate rocks according to depositional texture. *In* W.E. Ham (ed.), *Classification of carbonate rocks*. Memoir - American Association of Petroleum Geologists, **1**. American Association of Petroleum Geologists, Tulsa, 108-121.

DUPRAZ C., REID R.P., BRAISSANT O., DECHO A.W., NORMAN R.S. & VISSCHER P.T., 2009 - Processes of carbonate precipitation in modern microbial mats. *Earth-Science Reviews*, **96**, 141-162.

ERTHAL M.M., CAPEZZUOLI E., MANCINI A., CLAES H., SOETE J. & SWENNEN R., 2017 - Shrub morpho-types as indicator for the water flow energy - Tivoli travertine case (Central Italy). *Sedimentary Geology*, **347**, 79-99.

FOLK R.L. & CHAFETZ H.S., 1983 - Pisoliths (pisoids) in Quaternary travertines of Tivoli, ltaly. *In* T.M. Peryt, (ed.), *Coated Grains*. Springer Verlag, New York, 474-487.

FOLK R.L., CHAFETZ H.S. & TIEZZI P.A., 1985 - Bizarre forms of depositional and diagenetic calcite in hot-spring travertines, central Italy. *Special publication - Society of Economic Paleontologists and Mineralogists*, **36**, 349-369.

FORD T.D. & PEDLEY H.M., 1996 - A review of tufa and travertine deposits of the World. *Earth-Science Review*, **41**, 117-175.

FORT M., BURBANK D.W. & FREYTET P., 1989 - Lacustrine sedimentation in a semi-arid alpine setting: an example from Ladakh, Northwestern Himalayas. *Quaternary Research*, **31**, 332-350.

FREYTET P. & VERRECCHIA E.P., 2002 - Lacustrine and palustrine carbonate petrography: an overview. *Journal of Paleolimnology*, **27** (2), 221-237.

GANDIN A. & CAPEZZUOLI E., 2014 - Travertine: Distinctive depositional fabrics of carbonates from thermal spring systems. *Sedimentology*, **61**, 264-290.

GIERLOWSKI-KORDESCH, E.H., 2010 - Lacustrine carbonates. *In* A.M. Alonso-Zarza & L.H. Tanner (eds.), *Carbonates in continental settings: Facies, environments and processes*. Developments in Sedimentology, **61**. Elsevier, Amsterdam, 17-18.

GOLDENFELD N., CHAN P.Y. & VEYSEY J., 2006 - Dynamics of precipitation pattern formation at geothermal hot springs. *Physical Review Letters*, **96**, 1-4.

GUO L. & RIDING R., 1992 - Microbial micritic carbonates in uppermost Permian reefs, Sichuan Basin, southern China: some simiraties with Recent travertines. *Sedimentology*, **39**, 37-53.

GUO L. & RIDING R., 1994 - Origin and diagenesis of Quaternary travertine shrub fabrics, Rapolano Terme, central Italy. *Sedimentology*, **41**, 499-520.

GUO L. & RIDING R., 1998 - Hot-spring travertine facies and sequences, Late Pleistocene, Rapolano Terme, Italy. *Sedimentology*, **45**, 163-180.

HERLINGER R., ZAMBONATO E.E. & LOS L.F.D., 2017 - Influence of Diagenesis on The Quality of Lower Cretaceous Pre-Salt Lacustrine Carbonate Reservoirs from Northern Campos Basin, Offshore Brazil. *Journal of Sedimentary Research*, **87**, 1285-1313.

JAHNERT R.J. & COLLINS L.B., 2013 - Controls on microbial activity and tidal flat evolution in Shark Bay, Western Australia. *Sedimentology*, **60**, 1071-1099.

JONES B. & RENAUT R.W., 1995 - Noncrystallographic calcite dendrites from hot-spring deposits at Lake Bogoria, Kenya. *Journal of Sedimentary Research*, **65** (1a), 154-169.

JONES B., RENAUT R.W., OWEN B.R. & TORFASON H., 2005 - Growth patterns and implications of complex dendrites in calcite travertines from L suhóll, Snæfellsnes, Iceland. *Sedimentology*, **52**, 1277-1301.

KAYMAKÇI N., 2006 - Kinematic development and paleostress analysis of the Denizli Basin (Western Turkey): implications of spatial varition of relative paleostress magnitudes and orientations. *Journal of Asian Earth Sciences*, **27**, 207-222.

KELE S., ÖZKUL M., FORIZS I., GÖKGÖZ A., BAYKARA M.O., ALÇİÇEK M.C. & NEMETH T., 2011 - Stable isotope geochemical and facies study of Pamukkale travertines: new evidences of low temperature non-equilibrium calcite-water fractionation. *Sedimentary Geology*, **238**, 191-212.

KLAPPA C.F., 1978 - Biolithogenesis of Microcodium: elucidation. *Sedimentology*, **25**, 489-522.

KOÇYİĞİT A., 2005 - The Denizli graben-horst system and the eastern limit of western Anatolian continental extension: basin-fill, structure, deformational mode, throw amount and episodic evolutionary history, SW Turkey. *Geodinamica Acta*, **18**, 167-208.

LIMA B.E.M. & ROS L.F.D., 2019 - Deposition, diagenetic and hydrothermal processes in the Aptian Pre-Salt lacustrine carbonate reservoirs of the northern Campos Basin, offshore Brazil. *Sedimentary Geology*, **383**, 55-81.

LIMA B.E.M., TEDESCHI L.R., PESTILHO A.L.S., SANTOS R.V., VAZQUEZ J.C., GUZZO J.V.P. & ROS L.F.D., 2020 - Deep-burial hydrothermal alteration of the Pre-Salt carbonate reservoirs from northern Campos Basin, offshore Brazil: Evidence from petrography, fluid inclusions, Sr, C and O isotopes. *Marine and Petroleum Geology*, **113**, 104-143.

LIPPMANN F., 1973 - *Sedimentary carbonate minerals*. Springer-Verlag, Berlin, 228 p.

LØNØY A., 2006 - Making sense of carbonate pore systems. *AAPG Bulletin*, **90**, 1381-1405.

LOPEZ B., CAMOIN G., ÖZKUL M., SWENNEN R. & VIRGONE A., 2017 - Sedimentology of coexisting travertine and tufa deposits in a mounded geothermal spring carbonate system, Obrukhill, Turkey. *Sedimentology*, **64**, 903-931.

MARTIN-ALGARRA A., MARTIN-MARTIN M., ANDREO B., JULIA R. & GONZALEZ-GOMEZ C., 2003 - Sedimentary patterns in perched spring travertines near Granda (Spain) as indicators of the paleohydrological and paleoclimatological evolution of a karst massif. *Sedimentary Geology*, **161**, 217-228.

MOHAMMADI Z., CLAES H., CAPEZZUOLI E., MOZAFARI M., SOETE J., ARATMAN C. & SWENNEN R., 2020 - Lateral and vertical variations in sedimentology and geochemistry of sub-horizontal laminated travertines (Çakmak quarry, Denizli Basin, Turkey). *Quaternary International*, **540**, 146-168.

OKUMURA T., TAKASHIMA C., SHIRAISHI F., AKMALUDDIN & KANO A., 2012 - Textural transition in an aragonite travertine formed under various flow conditions at Pancuran Pitu, Central Java, Indonesia. *Sedimentary Geology*, **265-266**, 195-209.

ORHAN H. & KALAN F., 2015 - Sedimentological characteristics of Quaternary Aydıncık Tufa (Mersin-Turkey). *Carbonates Evaporites*, **30**, 451-459.

ÖZKUL M., VAROL B. & ALÇİÇEK M.C., 2002 - Depositional environments and petrography of Denizli travertines. *Bulletin of The Mineral Research and Exploration*, **125**, 13-29.

ÖZKUL M., GÖKGÖZ A. & HORVATINCIC N., 2010 - Depositional properties and geochemistry of Holocene perched springline tufa deposits and associated spring waters: a case study from the Denizli province, Western Turkey. *In* H.M. Pedley & M. Rogerson (eds.), *Tufas and Speleothems: Unravelling the Microbial and Physical Controls*. Geological Society, London, **336**. Geological Society of London, London, 245-262.

ÖZKUL M., KELE S., GÖKGÖZ A., SHEN C.C., JONES B., BAYKARA M.O., FORIZS I., NEMETH T., CHANG Y.-W. & ALÇİÇEK M.C., 2013 - Comparison of the Quaternary travertine sites in the Denizli Extensional Basin based on their depositional and geochemical data. *Sedimentary Geology*, **294**, 179-204.

ÖZKUL M., GÖKGÖZ A., KELE S., BAYKARA M.O., SHEN C.-C., CHANG Y.-W., KAYA A., HANÇER M., ARATMAN C., AKIN T. & ÖRÜ Z., 2014 - Sedimentological and geochemical characteristics of a fluvial travertine: a case from the eastern Mediterranean region. *Sedimentology*, **61**, 291-318.

PEDLEY M., 1990 - Classification and environmental models of cool freshwater tufas. *Sedimentary Geology*, **68**, 143-154.

PEDLEY M., 2009 - Tufas and travertines of the Mediterranean region: a testing ground for freshwater carbonate concepts and developments. *Sedimentology*, **56**, 221-246.

PEDLEY H.M., DENTON H.P. & BRASINGTON J., 2000 - Three-dimensional modelling of a Holocene tufa system in the Lathkill Valley, north Derbyshire, using ground-penetrating radar. *Sedimentology*, **47**, 721-737.

PEDLEY M., GONZALEZ-MARTIN J.A., ORDONEZ D.S. & GARCIA D.C.M.A., 2003 - Sedimentology of Quaternary perched springline and paludal tufas: criteria for recognition, with examples from Guadalajara Province, Spain. *Sedimentology*, **50**, 23-44.

PENTECOST A., 2005 - Travertine. Springer, Berlin, 445 p.

PENTECOST A. & VILES H., 1994 - A review and reassessment of travertine classification. *Géographie Physique et Quaternaire*, **48** (3), 305-314.

PERTUSATI P.C., MUSUMECI G., BONINI L. & TRUMPY E., 2004 - *Carta Geologica della Toscana, 1:10000, sezione 343050-Manciano*.

PENTECOST A. & ZHAOHUI Z., 2002 - Bryophytes from some travertine-depositing sites in France and the U.K.: relationships with climate and water chemistry. *Journal of Bryology*, **24**, 233-241.

RAINEY D.K. & JONES B., 2009 - Abiotic versus biotic controls on the development of the Fairmont Hot Springs carbonate deposit, British Columbia, Canada. *Sedimentology*, **56**, 1832-1857.

REZENDE M.F., TONIETTO S.N. & POPE M.C., 2013 - Three-dimensional pore connectivity evaluation in a Holocene and Jurassic microbialite buildup. *AAPG Bulletin*, **97**, 2085-2101.

ROSSI C. & CAÑAVERAS J.C., 1999 - Pseudospherulitic fibrous calcite in paleo-groundwater, unconformity-related diagenetic carbonates (Paleocene of the Ager Basin and Miocene of the Madrid Basin, Spain). *Journal of Sedimentary Research*, **69**, 224-238.

SALLER A.H., BUDD D.A. & HARRIS P.M., 1994 - Unconformities and porosity developments in carbonate strata: Ideas from a Hedberg Conference1. *AAPG Bulletin*, **78**, 857-872.

SALLER A.H, RUSHTON S., BUAMBUA L., INMAN K., MCNEIL R. & DICKSON J.A.D. (TONY), 2016 - Presalt stratigraphy and depositional systems in the Kwanza Basin, offshore Angola. *AAPG Bulletin*, **100**, 1135-1164.

SEMENIUK V. & MEAGHER T.D., 1981 - Calcrete in Quaternary coastal dunes in southwestern australia: a capillary-rise phenomenon associated with plants. *Journal of Sedimentary Research*, **51**, 47-68.

SWENNEN R., ARATMAN C., CAPEZZUOLI E., CLAES H., ERTHAL M.M., JANSSENS N., KELE S., MANCINI A., MOHAMMADI Z., ÖZKUL M., SOETE J., TOROK A. & VERBIEST M. – The use of reservoir analogues to better constrain geobody architecture, genesis, and petrophysical characteristics of continental carbonates. *AAPG|SEG International Conference and Exhibition, 15th-18th October 2017, London, England*.

ŞİMŞEK S., GÜNAY G., ELHATIP H. & EKMEKÇI M. 2000 - Environmental protection of geothermal waters and travertines at Pamukkale, Turkey, *Geothermics*, **29**, 557–572.

TERRA G.J.S., SPADINI A.R., FRANCA A.B., SOMBRA C.L., ZAMBONATO E.E., JUSCHAKS L.C.D.S., ARIENTI L.M., ERTHAL M.M., BLAUTH M., FRANCO P.P., MATSUDA N.S., DA SILVA N.G.C., JUNIOR P.A.M., D'AVILA R.S.F., DESOUZA R.S., TONIETTO S.N., DOS ANJOS S.M.C., CAMPINHO V.S. & WINTER W.R., 2010 - Classificac~ao de rochas carbonaticasaplicacavel as bacias sedimentares brasileiras. Carbonate rock classification applied to brazilian sedimentary basins. *Boletim de Geociências da Petrobras*, **18**, 9-29.

TOKER E., KAYSERİ-ÖZER M.S., ÖZKUL M. & KELE S., 2015 - Depositional system and palaeoclimatic interpretations of Middle to Late Pleistocene travertines: Kocabas, Denizli, sout-west Turkey. *Sedimentology*, **62**, 1360-1383.

TOKER E., 2016 - Quaternary fluvial tufas of Sarikavak area, southwestern Turkey: Facies and depositional systems. *Quaternary International*, **437**, 37-50.

UYSAL I.T., FENG Y., ZHAO J., ALTUNEL E., WEATHERLEY D., KARABACAK V., CENGİZ O., GOLDING S.D., LAWRENCE M.G. & COLLERSON K.D., 2007 - U-Series dating and geochemical tracing of late Quaternary travertine in coseismic fissures. *Earth and Planetary Science Letters*, **257**, 450-462.

VAN NOTEN K., CLAES H., SOETE J., FOUBERT A., ÖZKUL M. & SWENNEN R., 2013 - Fracture networks and strike–slip deformation along reactivated normal faults in Quaternary travertine deposits, Denizli Basin, western Turkey. *Tectonophysics*, **588**, 154-170.

VAN NOTEN K., TOPAL S., BAYKARA M.O., ÖZKUL M., CLAES H., ARATMAN C. & SWENNEN R., 2019 - Pleistocene-Holocene tectonic reconstruction of the Ballık travertine (Denizli Graben, SW Turkey): (de)formation of large travertine geobodies at intersecting grabens. *Journal of Structural Geology*, **118**, 114-134.

VAZQUEZ-URBEZ M., ARENAS C. & PARDO G., 2012 - A sedimentary facies model for stepped, fluvial tufa systems in the Iberian Range (Spain): the Quaternary Piedra and Mesa valleys. *Sedimentology*, **59**, 502-526.

VIOLANTE C., FERRERI V., D'ARGENIO B. & GOLUBIC S., 1994 - Quaternary travertines at Rochetta a Volturno (Isernia, Central Italy). Facies analysis and sedimentary model of an organogenic carbonate system. *In PreMeeting Fieldtrip Guidebook, A1, International Association of Sedimentologists, Ischia'94, 15th Regional Meeting, Italy*. 3223.

VOLERY C., DAVAUD E., FOUBERT A. & CALINE B., 2010 - Lacustrine microporous micrites of the Madrid Basin (Late Miocene, Spain) as analogues for shallow-marine carbonates of the Mishrif reservoir Formation (Cenomanian to Early Turonian, Middle East). *Facies*, **56**, 385-397.

WESTAWAY R., GUILLOU H., YURTMEN S., DEMIR T., SCAILLET S. & ROWBOTHAM G., 2005 - Investigation of the conditions at the start of the present phase of crustal extension in western Turkey, from observations in and around the Denizli region. *Geodinamica Acta*, **18**, 209-238.

WEIJERMARS R., MULDER-BLANKEN C.W. & WIEGERS J., 1986 - Growth rate observation from the moss-built Checa travertine terrace, central Spain. *Geological Magazine*, **123**, 279-286.

WRIGHT V.P., 2012 - Lacustrine carbonates in rift settings: The interaction of volcanic and microbial processes on carbonate deposition. *Special publication - Geological Society of London*, **370**, 1-39.

WRIGHT, V.P. & BARNETT, A.J., 2015 - An abiotic model for the development of textures in some South Atlantic early Cretaceous lacustrine carbonates. *In* D.W.J. Bosence, K.A. Gibbons, D.P. Le Heron, W.A. Morgan, T. Pritchard, B.A. Vining (eds.), *Microbial Carbonates in Space and Time: Implications for Global Exploration and Production*. Special Publications - Geological Society, **418**. Geological Society of London, London, 209-219.

ZHANG D.D., ZHANG Y., ZHU A. & CHENG X., 2001 - Physical mechanisms of river waterfall tufa (travertine) formation. *Journal of Sedimentary Research*, *71*, 205-216.